[34] Kagota S, Tada Y, Nejime N, Nakamura K, Kunitomo M, Shinozuka K. Telmisartan provides protection against development of impaired vasodilation independently of metabolic effects in SHRSP.Z-Lepr(fa)/IzmDmcr rats with metabolic syndrome. Can J Physiol Pharmacol 2011;89:355–64.
[35] Kishi T, Hirooka Y, Sunagawa K. Sympathoinhibition caused by orally administered telmisartan through inhibition of the AT1 receptor in the rostral ventrolateral medulla of hypertensive rats. Hypertens Res 2012, http://dx.doi.org/10.1038/hr.2012.63. May 10 [Epub ahead of print].
[36] Morris R. Development of a water-maze procedure for studying spatial learning in the rat. J Neurosci Methods 1984;11:47–60.
[37] Kobayashi N, Ohno T, Yoshida K, Fukushima H, Mamada Y, Nomura M, Hirata H, Machida Y, Shinoda M, Suzuki N, Matsuoka H. Cardioprotective mechanism of telmisartan via PPAR-γ-eNOS pathway in Dahl salt-sensitive hypertensive rats. Am J Hypetens 2008;21:576–81.
[38] Wagner J, Drab M, Bohlender J, Amann K, Wienen W, Ganten D. Effects of AT1 receptor blockade on blood pressure and the renin–angiotensin system in spontaneously hypertensive rats of the stroke prone strain. Clin Exp Hypertens 1998;20:205–21.
[39] Cazorla M, Prémont J, Mann A, Girard N, Kellendonk C, Rognan D. Identification of a low-molecular weight TrkB antagonist with anxiolytic and antidepressant activity in mice. J Clin Invest 2011;121:1846–57.
[40] Beck T, Lindholm D, Castren E, Wree A. Brain-derived neurotrophic factor protects against ischemic cell damage in rat hippocampus. J Cereb Blood Flow Metab 1994;14:689–92.
[41] Denny JB, Polan-Curtain J, Wayner MJ, Armstrong DL. Angiotensin II blocks hippocampal long-term potentiation. Brain Res 1991;567:321–4.
[42] Wayner MJ, Armstrong DL, Polan-Curtain JL, Denny JB. Role of angiotensin II and AT1 receptors in hippocampal LTP. Pharmacol Biochem Behav 1993;45:455–64.
[43] Gard PR. The role of angiotensin II in cognition and behavior. Eur J Pharmacol 2002;438:1–14.
[44] De Bundel D, Demaegdt H, Lahoutte T, Cavelier V, Kersemans K, Ceulemans AG, Vauquelin G, Clinckers R, Vanderheyden P, Michotte Y, Smolders I. Involvement of the AT1 receptor subtype in the effects of angiotensin IV and LVVhaemorphin 7 on hippocampal neurotransmitter levels and spatial working memory. J Neurochem 2010;112:1223–34.
[45] Berr C, Balansard B, Arnaud J, Roussel AM, Alperovitch A. Cognitive decline is associated with systemic oxidative stress: the EVA study. Etude du Vieillissement Arterial. J Am Geriatr Soc 2000;48:1285–91.
[46] Sato H, Takahashi T, Sumitani K, Takatsu H, Urano S. Glucocorticoid generates ROS to induce oxidative injury in the hippocampus, leading to impairment of cognitive function of rats. J Clin Biochem Nutr 2010;47:224–32.
[47] Saxby BK, Harrington F, Wesnes KA, McKeith IG, Ford GA. Candesartan and cognitive decline in older patients with hypertension a substudy of the SCOPE trial. Neurology 2008;70:1858–66.
[48] Toda S, Kamat PK, Awasthi H, Singh N, Raghubir R, Nath C, Hanif K. Candesartan improves memory decline in mice: involvement of AT1 receptors in memory deficit induced by intracerebral streptozotocin. Behave Brain Res 2009;199:235–40.
[49] Li NC, Lee A, Whitmer RA, Kivipelto M, Lawler E, Kazis LE, Wolozin B. Use of angiotensin receptor blockers and risk of dementia in a predominantly male population: prospective cohort analysis. BMJ 2010;340:b5465.
[50] Kim-Mitsuyama S, Yamamoto E, Tanaka E, Zhan Y, Izumiya Y, Ioroi T, Wanibuchi H, Iwao H. Critical role of angiotensin II in excess salt-induced brain oxidative stress of stroke-prone spontaneously hypertensive rats. Stroke 2005;36:1083–8.
[51] Hirooka Y, Sagara Y, Kishi T, Sunagawa K. Oxidative stress and central cardiovascular regulation. Pathogenesis of hypertension and therapeutic aspects-. Circ J 2010;74:827–35.
[52] Tsuchihashi T, Kagiyama S, Matsumura K, Abe I, Fujishima M. Effects of chronic oral treatment with imidapril and TCV-116 on the responsiveness to angiotensin II in ventrolateral medulla of SHR. J Hypertens 1999;17:917–22.
[53] Pelosch N, Hosomi N, Ueno M, Masugata H, Murao K, Hitomi H, Nakao D, Kobori H, Nishiyama A, Kohno M. Systemic candesartan reduces brain angiotensin II via downregulation of brain renin–angiotensin system. Hypertens Res 2010;33:161–4.
[54] Ueno M, Sakamoto H, Liao YJ, Onodera M, Huang CL, Miyanaka H, Nakagawa T. Blood–brain barrier disruption in the hypothalamus of young adult spontaneously hypertensive rats. Histochem Cell Biol 2004;122:131–7.
[55] Lippoldt A, Kniesel U, Liebner S, Kalbacher H, Kirsch T, Wolburg H, Haller H. Structural alterations of tight junctions are associated with loss of polarity in stroke-prone spontaneously hypertensive rat blood–brain barrier endothelial cells. Brain Res 2000;885:251–61.
[56] Gohlke P, Weiss S, Jansen A, Wienen W, Stangier J, Rascher W, Culman J, Unger T. AT1 receptor antagonist telmisartan administered peripherally inhibits central responses to angiotensin II in conscious rats. J Pharmacol Exp Ther 2001;298:62–70.
[57] Maillard MP, Perregaux C, Centeno C, Stangier J, Wienen W, Brunner HR, Burnier M. In vitro and in vivo characterization of the activity of telmisartan: an insurmountable angiotensin II receptor antagonist. J Pharmacol Exp Ther 2002;302:1089–95.
[58] Moser MB, Trommald M, Andersen P. An increase in dendritic spine density on hippocampal CA1 pyramidal cells following spatial learning in adult rats suggests the formation of new synapses. Proc Natl Acad Sci U S A 1994;91:12673–5.
[59] Barnes CA. Spatial learning and memory processes: the search for their neurobiological mechanisms in the rat. Trends Neurosci 1988;11:163–9.
[60] Gahring LC, Persiyanov K, Days EL, Rogers SW. Age-related loss of neuronal nicotinic receptor expression in the aging mouse hippocampus corresponds with cyclooxygenase-2 and PPAR-gamma expression and is altered by long-term NS398 administration. J Neurobiol 2005;62:453–68.
[61] Wang D, Hirase T, Nitto T, Soma M, Node K. Eicosapentaenoic acid increases cytochrome P-450 2J2 gene expression and epoxyeicosatrienoic acid production via peroxisome proliferator-activated receptor γ in endothelial cells. J Cardiol 2009;54:368–74.

Original Article

Sympathoinhibitory effects of telmisartan through the reduction of oxidative stress in the rostral ventrolateral medulla of obesity-induced hypertensive rats

Satomi Konno[a], Yoshitaka Hirooka[b], Takuya Kishi[c], and Kenji Sunagawa[a]

Objectives: Sympathetic nervous system (SNS) activity is critically involved in the development and progression of obesity-induced hypertension. Angiotensin II type 1 receptor (AT_1R)-induced oxidative stress in the rostral ventrolateral medulla (RVLM), a vasomotor center in the brainstem, activates the SNS in hypertensive rats. The aim of the present study was to determine whether oral administration of an AT_1R blocker (ARB) inhibits SNS activity via antioxidative effects in the RVLM of rats with dietary-induced obesity.

Methods and results: Obesity-prone rats fed a high-fat diet were divided into groups treated with either telmisartan obesity-prone (TLM-OP), or losartan obesity-prone (LOS-OP), or vehicle obesity-prone (VEH-OP). SBP, SNS activity, and oxidative stress in the RVLM were significantly higher in obesity-prone rats than in obesity-resistant rats. Body weight, visceral fat, blood glucose, serum insulin, and plasma adiponectin concentrations were significantly lower in TLM-OP and LOS-OP than in VEH-OP, and plasma adiponectin concentrations were significantly higher in TLM-OP than in LOS-OP. Although SBP was reduced to similar levels both in TLM-OP and LOS-OP, both oxidative stress in the RVLM and SNS activity were significantly lower in TLM-OP than in LOS-OP or VEH-OP.

Conclusion: Orally administered telmisartan inhibited SNS activity through antioxidative effects via AT_1R blockade in the RVLM of obesity-prone rats. AT_1R and oxidative stress in the RVLM might be novel treatment targets for obesity-induced hypertension through sympathoinhibition, and telmisartan might be preferable for obesity-induced hypertension.

Keywords: angiotensin II, brain, hypertension, obesity, sympathetic nervous system

Abbreviations: ARBs, angiotensin II receptor blockers; AT_1R, angiotensin II type 1 receptor; MetS, metabolic syndrome; NAD (P) H, nicotinamide adenine dinucleotide phosphate; PPAR, peroxisome proliferator-activated receptor; RVLM, rostral ventrolateral medulla; SNS, sympathetic nervous system; TBARS, thiobarbituric acid-reactive substances

INTRODUCTION

Metabolic syndrome (MetS) is characterized by the presence of central obesity, impaired fasting glucose, dyslipidemia, and obesity-induced hypertension [1–3]. Previous studies indicated that sympathetic nervous system (SNS) activity is involved in the development and progression of obesity-induced hypertension [4–8]. SNS activity is mediated by the rostral ventrolateral medulla (RVLM), a major vasomotor center in the brainstem, and the functional integrity of the RVLM is essential for the maintenance of basal vasomotor tone [9,10]. Neurons in the RVLM contribute to elevated sympathetic outflow in rats with dietary-induced obesity [11]. We previously demonstrated that oxidative stress in the RVLM produced by activation of angiotensin II type 1 receptors (AT_1R) increases SNS activity [12–14]. In obesity-induced hypertension, oxidative stress is increased and is associated with the development and progression of hypertension in various organs [15–18]. Oxidative stress in the hypothalamus contributes to the progression of obesity-induced hypertension through central sympathoexcitation [19]. Moreover, AT_1R-induced oxidative stress in the RVLM induces sympathoexcitation in rats with obesity-induced hypertension [20]. Direct microinjection of AT_1R blockers (ARBs) into the RVLM or intracerebroventricular infusion of ARBs inhibits SNS activity in hypertensive rats [13,21–23]. Orally administered telmisartan inhibits SNS activity by blocking AT_1R in the brain of hypertensive rats [14]. Further, orally administered telmisartan inhibits the central responses to angiotensin II, and peripherally administered telmisartan penetrates the blood–brain barrier in a dose-dependent and time-

Journal of Hypertension 2012, 30:1992–1999

[a]Department of Cardiovascular Medicine, [b]Department of Advanced Cardiovascular Regulation and Therapeutics and [c]Department of Advanced Therapeutics for Cardiovascular Diseases, Kyushu University Graduate School of Medical Sciences, Fukuoka, Japan

Correspondence to Yoshitaka Hirooka, MD, PhD, FAHA, Department of Advanced Cardiovascular Regulation and Therapeutics, Kyushu University Graduate School of Medical Sciences, 3-1-1 Maidashi, Higashi-ku, Fukuoka 812-8582, Japan. Tel: +81 92 642 5356; fax: +81 92 642 5374; e-mail: hyoshi@cardiol.med.kyushu-u.ac.jp

Received 29 February 2012 **Revised** 22 May 2012 **Accepted** 10 July 2012

J Hypertens 30:1992–1999

DOI:10.1097/HJH.0b013e328357fa98

dependent manner to inhibit the centrally mediated effects of angiotensin II [24]. Although other ARBs also inhibit the central actions of angiotensin II in the brain [24–29], these effects might differ depending on the pharmacokinetics and properties of each drug [24]. It is not known, however, whether orally administered telmisartan blocks AT_1R in the RVLM in obesity-induced hypertension, and if so, whether these are class effects of ARBs.

In the present study, we divided obesity-induced hypertensive rats into three treatment groups receiving either telmisartan, losartan, or vehicle. In hypertensive patients, renin–angiotensin inhibitors, such as angiotensin-converting enzyme inhibitors and ARBs, are preferable for the treatment of hypertension in patients with MetS [30,31]. SNS activity was determined by 24-h urinary norepinephrine excretion and oxidative stress in the RVLM was measured using the thiobarbituric acid-reactive substances (TBARS) method. We also examined the activity of nicotinamide adenine dinucleotide phosphate [NAD (P) H] oxidase, which is the key AT_1R-activated component in the production of oxidative stress in the RVLM [13,32]. Furthermore, we microinjected losartan, angiotensin II, a superoxide dismutase mimetic (tempol), or NAD (P) H oxidase inhibitor (apocynin) into the RVLM of each group.

METHODS

Animals

This study was reviewed and approved by the committee on the ethics of Animal Experiments, Kyushu University Graduate School of Medical Sciences, and conducted according to the Guidelines for Animal Experiments of Kyushu University. Male Sprague–Dawley rats (Charles River Laboratories, Kingston, New York, USA) weighing 350–425 g were individually housed in a temperature-controlled room (22–23°C) with a 12-h/12-h light–dark cycle (lights on at 0700 h). The rats were placed on a moderate high-fat diet (32% kilocalorie from fat; Research Diets, New Brunswick, New Jersey, USA) for 13 weeks. After 5 weeks, rats fed the moderately high-fat diet were classified as obesity-prone or obesity-resistant based on the body weight distribution, as described previously [11,20]. Briefly, a body weight histogram was constructed to show the distribution of the rats; rats falling within the upper third of the weight distribution were classified as obesity prone ($n = 40$) and those falling within the lower third were classified as obesity resistant ($n = 10$) [11,20].

Oral administration of telmisartan or losartan to obesity-prone rats

Of the 40 obesity-prone rats, 10 rats were used for the obesity-prone-only group, and the remaining 30 rats were divided into three groups and treated with either telmisartan obesity-prone (TLM-OP, $n = 10$), losartan obesity-prone (LOS-OP, $n = 10$), or vehicle obesity-prone (VEH-OP, $n = 10$). The TLM-OP group was orally administered telmisartan (5 mg/kg per day; Sigma Aldrich, St. Louis, Missouri, USA) dissolved in 0.3% methylcellulose with a pellet once daily. The LOS-OP group was orally administered losartan (30 mg/kg per day; Sigma Aldrich) in the drinking water for 12 weeks. Food was given to all groups daily 2–3 h before lights-off. Doses of telmisartan and losartan were selected to produce comparable antihypertensive effects based on earlier reports [33,34].

Measurement of blood pressure, heart rate, and sympathetic nervous system activity

SBP and heart rate were measured using the tail-cuff method (BP-98A; Softron, Tokyo, Japan). We calculated the 24-h urinary norepinephrine excretion as an indicator of SNS activity, as described previously [12,13].

Microinjection of losartan, angiotensin II, tempol, or apocynin into the rostral ventrolateral medulla

In the acute experiments, drugs were microinjected under anesthesia (sodium pentobarbital, 50 mg/kg intraperitoneally followed by 2 mg/kg per hour intravenously) in five rats from each group. Blood pressure and heart rate were measured through a catheter inserted into the femoral artery as described previously [12,13]. Prior to the microinjection, blood samples were collected from the arterial line. Each drug was microinjected after blood pressure and heart rate recovered to the basal levels. To inhibit AT_1R, oxidative stress, and NAD (P) H oxidase in the RVLM locally, we microinjected losartan (1 nmol), tempol (100 pmol), and apocynin (1 nmol), respectively, into the bilateral RVLM of obesity-prone and obesity-resistant rats, and in TLM-OP, LOS-OP, and VEH-OP rats. Furthermore, we microinjected angiotensin II into the bilateral RVLM of obesity-prone and obesity-resistant rats, and into TLM-OP, LOS-OP, and VEH-OP rats at the end of this study. After all of the microinjections, we measured the visceral fat, including retroperitoneal, epididymal, and total mesenteric fats.

Measurement of thiobarbituric acid-reactive substances in the rostral ventrolateral medulla

To obtain the RVLM tissues, the rats were deeply anesthetized with sodium pentobarbital (100 mg/kg intraperitoneally) and perfused transcardially with PBS (150 mol/l NaCl, 3 mmol/l KCl, and 5 nmol/l phosphate; pH 7.4, 4°C). The brains were removed quickly, and 1-mm thick coronal sections were obtained with a cryostat at -7 ± 1°C. The RVLM was defined according to a rat brain atlas as described previously [12], and obtained using a punch-out technique. The RVLM tissues were homogenized in 1.15% KCl (pH 7.4) and 0.4% sodium dodecyl sulfate, 7.5% acetic acid adjusted to pH 3.5 with NaOH. Thiobarbituric acid (0.3%) was added to the homogenate. The mixture was maintained at 5°C for 60 min, followed by heating to 100°C for 60 min. After cooling, the mixture was extracted with distilled water and *n*-butanolpyridine (15 : 1) and centrifuged at 1600 *g* for 10 min. The absorbance of the organic phase was measured at 532 nm. The amount of TBARS was determined by absorbance, as described previously [12,13].

Measurement of nicotinamide adenine dinucleotide phosphate oxidase activity

NAD (P) H-dependent superoxide production in the RVLM was measured using a lucigenin luminescence assay as

TABLE 1. Metabolic profiles

	OP	OR	OP		
			TLM	LOS	VEH
n	5	5	5	5	5
Body weight (g)	788 ± 43*	602 ± 38	795 ± 28+	812 ± 30+	887 ± 32
Visceral fat (g)	68 ± 8*	32 ± 11	57 ± 9+	65 ± 10+	86 ± 12
Caloric intake (kcal/day)	113 ± 9*	80 ± 7	106 ± 10	102 ± 11	109 ± 8
Fasting BG (mg/dl)	92 ± 5*	81 ± 6	86 ± 4+	88 ± 3+	96 ± 5
Fasting BI (ng/ml)	1.2 ± 0.2*	0.3 ± 0.1	0.6 ± 0.1+	0.8 ± 0.2+	1.4 ± 0.2
Adiponectin (μg/ml)	1.7 ± 0.2*	2.5 ± 0.3	2.2 ± 0.2+,#	1.8 ± 0.2+	1.5 ± 0.2
Serum TG (mg/dl)	94 ± 7*	64 ± 8	71 ± 9+	76 ± 8+	98 ± 7
Serum FFA (μmol/l)	688 ± 72*	326 ± 85	524 ± 103+	562 ± 93+	724 ± 84

BG, blood glucose; BI, blood insulin; FFA, free fatty acid; LOS, losartan; OP, obesity-prone rats; OR, obesity-resistance rats; TG, triglyceride; TLM, telmisartan; VEH, vehicle.
*$P < 0.05$ vs. OR in OP
+$P < 0.05$ vs. VEH in TLM or LOS
#$P < 0.05$ vs. LOS in TLM

described previously [13,32]. Quantification of NAD (P) H oxidase activity was expressed relative to that in obesity-resistant rats, which was assigned a value of 1.

Statistical analysis

All values are expressed as mean ± SEM. Comparisons between any two mean values were performed using Bonferroni's correction for multiple comparisons. Analysis of variance was used to compare all the parameters in the obesity-prone, obesity-resistant, TLM-OP, LOS-OP, and VEH-OP groups. Differences were considered to be statistically significant at a P value of less than 0.05.

RESULTS

Total body weight, visceral fat weight, and metabolic profiles of obesity-prone, obesity-resistant, and obesity-prone after treatment

Body weight, visceral fat weight, fasting blood glucose, and serum insulin were significantly higher in obesity-prone than in obesity-resistant, and significantly lower in both TLM-OP and LOS-OP than in VEH-OP after 12 weeks of treatment (Table 1). In TLM-OP and LOS-OP, the increases in body weight and visceral fat were attenuated during treatment (Table 1). Mean daily caloric intake was significantly higher in obesity-prone than in obesity-resistant. Mean daily caloric intake did not differ, however, between obesity-prone, TLM-OP, LOS-OP, and VEH-OP (Table 1). Plasma adiponectin concentrations were significantly lower in obesity-prone than in obesity-resistant, and significantly higher in both TLM-OP and LOS-OP than in VEH-OP after 12 weeks of treatment (Table 1). Plasma adiponectin concentrations were significantly higher in TLM-OP than in LOS-OP (Table 1).

Blood pressure, heart rate, urinary norepinephrine excretion of obesity-prone, obesity-resistant, and obesity-prone after treatment

SBP and heart rate were significantly higher in obesity-prone than in obesity-resistant, and significantly lower in both TLM-OP and LOS-OP than in VEH-OP after 12 weeks of treatment (Fig. 1a and b). SBP was not significantly different between TLM-OP and LOS-OP. Heart rate was significantly lower in TLM-OP than in LOS-OP (Fig. 1a and b). Urinary norepinephrine excretion was significantly higher in obesity-prone than in obesity-resistant, and significantly lower in TLM-OP than in VEH-OP after 12 weeks of treatment (Fig. 2). Urinary norepinephrine excretion did not differ significantly between LOS-OP and VEH-OP (Fig. 2).

Thiobarbituric acid-reactive substances levels and nicotinamide adenine dinucleotide phosphate oxidase activity in the rostral ventrolateral medulla of obesity-prone, obesity-resistant, and obesity-prone after treatment

TBARS levels in the RVLM were significantly higher in obesity-prone than in obesity-resistant, and significantly lower in TLM-OP than in VEH-OP after 12 weeks of treatment (Fig. 3a). TBARS levels in the RVLM were not significantly different between LOS-OP and VEH-OP (Fig. 3a). NAD (P) H oxidase activity in the RVLM was significantly higher in obesity-prone than in obesity-resistant, and significantly lower in TLM-OP than in VEH-OP after 12 weeks of treatment (Fig. 3b).

Effects of microinjection of angiotensin II or losartan into the rostral ventrolateral medulla of obesity-prone, obesity-resistant, and obesity-prone after treatment

In the anesthetized condition, basal mean arterial pressure (MAP) levels were significantly higher in obesity-prone

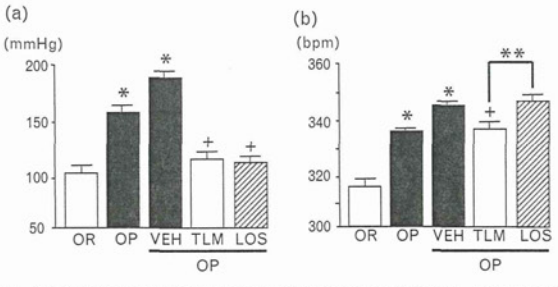

FIGURE 1 (a) SBP and (b) heart rate in obesity-prone (OP) rats, obesity-resistant (OR) rats, telmisartan (TLM)-treated OP rats, losartan (LOS)-treated OP rats, and vehicle (VEH)-treated OP rats ($n = 5$ per group). *, $P < 0.05$ vs. OR in OP or VEH; +, $P < 0.05$ vs. VEH in TLM or LOS; **, $P < 0.05$ vs. TLM in LOS.

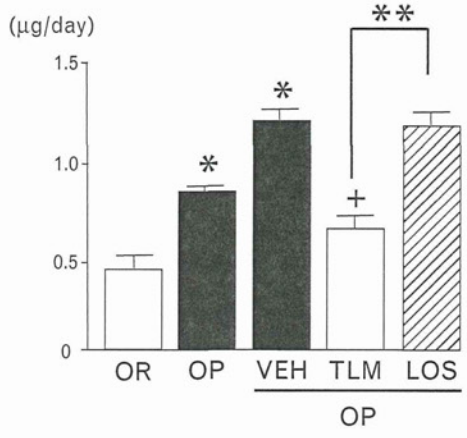

FIGURE 2 Twenty-four hour urinary norepinephrine excretion in obesity-prone (OP) rats, obesity-resistant (OR) rats, telmisartan (TLM)-treated OP rats, losartan (LOS)-treated OP rats, and vehicle (VEH)-treated OP rats ($n=5$ per group). *, $P<0.05$ vs. OR in OP or VEH; +, $P<0.05$ vs. VEH in TLM or LOS; **, $P<0.05$ vs. TLM in LOS.

than in obesity-resistant, and were significantly lower in both TLM-OP and LOS-OP than in VEH-OP (Table 2). Basal MAP levels were not significantly different between TLM-OP and LOS-OP (Table 2). Pressor effects caused by microinjection of angiotensin II into the RVLM were significantly greater in obesity-prone than in obesity-resistant (Fig. 4a; ΔMAP/basal MAP 11 ± 1 vs. $1\pm1\%$, $n=5$ for each, $P<0.01$) and significantly smaller in TLM-OP than in VEH-OP after 12 weeks of treatment (Fig. 4a; ΔMAP/basal MAP 5 ± 1 vs. $15\pm2\%$, $n=5$ for each, $P<0.01$). Pressor effects were not different between LOS-OP and VEH-OP (Fig. 4a; ΔMAP/basal MAP 17 ± 1 vs. $15\pm2\%$, $n=5$ for each).

Depressor effects caused by the microinjection of losartan into the RVLM were significantly greater in obesity-prone than in obesity-resistant (Fig. 4b; ΔMAP/basal MAP -10 ± 1 vs. $0\pm1\%$, $n=5$ for each, $P<0.01$), and significantly smaller in TLM-OP than in VEH-OP after 12 weeks of treatment (Fig. 4b; ΔMAP/basal MAP -8 ± 1 vs. $-15\pm2\%$, $n=5$ for each, $P<0.01$). Depressor effects were not different between LOS-OP and VEH-OP (Fig. 4b; ΔMAP/basal MAP -17 ± 2 vs. $-15\pm2\%$, $n=5$ for each).

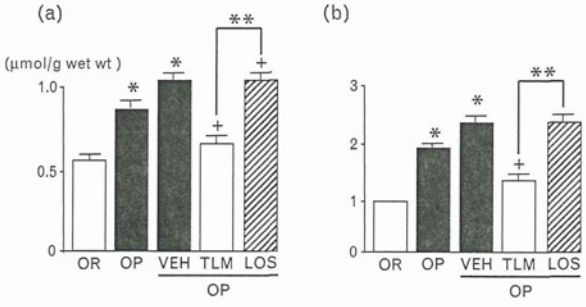

FIGURE 3 (a) Thiobarbituric acid-reactive substances levels and (b) nicotinamide adenine dinucleotide phosphate oxidase activity in the rostral ventrolateral medulla of obesity-prone (OP) rats, obesity-resistant (OR) rats, telmisartan (TLM)-treated OP rats, losartan (LOS)-treated OP rats, and vehicle (VEH)-treated OP rats ($n=5$ per group). *, $P<0.05$ vs. OR in OP or VEH; +, $P<0.05$ vs. VEH in TLM or LOS. **, $P<0.05$ vs. TLM in LOS.

Effects of microinjection of tempol or apocynin into the rostral ventrolateral medulla of obesity-prone, obesity-resistant, and obesity-prone after treatment

Depressor effects caused by microinjection of tempol into the RVLM were significantly greater in obesity-prone than in obesity-resistant (Fig. 5a; ΔMAP/basal MAP -9 ± 1 vs. $0\pm1\%$, $n=5$ for each, $P<0.01$), and significantly smaller in TLM-OP than in VEH-OP after 12 weeks of treatment (Fig. 5a; ΔMAP/basal MAP -7 ± 1 vs. $-19\pm2\%$, $n=5$ for each, $P<0.01$). Depressor effects were not different between LOS-OP and VEH-OP (Fig. 5a; ΔMAP/basal MAP -19 ± 1 vs. $-19\pm2\%$, $n=5$ for each).

Depressor effects caused by microinjection of apocynin into the RVLM were significantly greater in obesity-prone than in obesity-resistant (Fig. 5b; ΔMAP/basal MAP -8 ± 1 vs. $-1\pm1\%$, $n=5$ for each, $P<0.01$), and significantly smaller in TLM-OP than in VEH-OP after 12 weeks of treatment (Fig. 5b; ΔMAP/basal MAP -5 ± 1 vs. $-12\pm2\%$, $n=5$ for each, $P<0.01$). Depressor effects were not significantly different between LOS-OP and VEH-OP (Fig. 5b; ΔMAP/basal MAP -12 ± 1 vs. $-12\pm2\%$, $n=5$ for each).

DISCUSSION

The major novel findings of the present study are as follows. First, orally administered telmisartan decreased SNS activity by reducing oxidative stress due to blockade of AT_1R-NAD(P)H oxidase in the RVLM of obesity-induced hypertensive rats. Second, the sympathoinhibitory effects of orally administered telmisartan through the reduction of oxidative stress in the RVLM of obesity-induced hypertensive rats is not a class-effect of ARBs. These results indicate that orally administered telmisartan inhibits SNS activity by blocking AT_1R-NAD(P)H oxidase in the RVLM as well as metabolic profiles in obesity-induced hypertension.

In the present study, orally administered telmisartan, but not losartan, induced sympathoinhibition, despite their similar depressor effects. Together with the results regarding oxidative stress, NAD(P)H oxidase activity in the RVLM, and the pressor responses elicited by microinjection of angiotensin II into the RVLM, our findings suggest that AT_1R-NAD(P)H oxidase–oxidative stress in the RVLM is blocked by orally administered telmisartan, but not losartan. A previous study demonstrated that due to its high lipophilic properties, peripherally administered telmisartan penetrates the blood–brain barrier in a dose-dependent and time-dependent manner and inhibits the centrally mediated effects of angiotensin II [24]. We previously demonstrated that orally administered telmisartan inhibits SNS activity by blocking AT_1R in the brain of hypertensive rats [14]. Taken together, we consider that orally administered telmisartan (5 mg/kg per day) could penetrate the blood–brain barrier and inhibit AT_1R in the RVLM to a greater extent than orally administered losartan (30 mg/kg per day), despite the similar depressor effects. Although losartan also could penetrate the blood–brain barrier [25,35], the depressor effects caused by orally administered losartan are mainly due to direct blockade of AT_1R in the vasculature. Furthermore, previous studies

TABLE 2. Basal mean arterial pressure levels in anesthetized experiments

	OR	OP	OP		
			TLM	LOS	VEH
n	5	5	5	5	5
MAP (mmHg)	88 ± 2	107 ± 3*	96 ± 4+	98 ± 4+	114 ± 5

LOS, losartan; MAP, mean arterial pressure; OP, obesity-prone rats; OR, obesity-resistance rats; TLM, telmisartan; VEH, vehicle.
*$P < 0.05$ vs. OR in OP
+$P < 0.05$ vs. VEH in TLM or LOS

demonstrated differences between telmisartan and losartan [33,36–40]. Compared to losartan, telmisartan ameliorates vascular endothelial dysfunction to a greater degree via normalization of tumor necrosis factor-α activation [36]. Telmisartan shows insurmountable behavior, whereas losartan shows surmountable behavior [37]. In terms of inverse agonist activity, neither telmisartan nor losartan stabilize AT_1R in an inactive state in the absence of angiotensin II [38,39]. In terms of agonist activity of peroxisome proliferator-activated receptor (PPAR)-γ, a previous study suggested that orally administered rosiglitazone, a PPAR-γ agonist, promotes a central antihypertensive effect via upregulation of PPAR-γ and alleviation of oxidative stress in the RVLM of spontaneously hypertensive rats [40]. Although both telmisartan and losartan have a function as partial PPAR-γ agonists, only telmisartan achieves this effect in therapeutic doses [33,41]. Therefore, there is a possibility that the beneficial effects on the reduction of oxidative stress may differ among ARBs, and the differences between telmisartan and losartan on sympathoinhibition in obesity-induced hypertension might be related to differences in the antioxidant effects between the two compounds.

In the present study, AT_1R-NAD (P) H oxidase–oxidative stress in the RVLM contributed to sympathoexcitation in obesity-induced hypertensive rats, consistent with our previous study [20]. In the RVLM, oxidative stress is mainly produced by activation of AT_1R [13]. The central renin–angiotensin system mediates SNS activity via oxidative stress [13,32,42,43]. In the present study, we did not measure angiotensin II levels or AT_1R density in the RVLM. The depressor effect caused by microinjection of losartan, apocynin, or tempol into the RVLM, however, was significantly greater in obesity-prone than in obesity-resistant, and pressor effects of microinjection of angiotensin II into the RVLM were significantly greater in obesity-prone than in obesity-resistant. Based on the present and previous results, we consider that the mechanism by which obesity increases oxidative stress in the RVLM involves the activation of AT_1R-NAD (P) H oxidase–oxidative stress in the RVLM. Moreover, adipose tissue is reported to secrete angiotensinogen [44], and a PPAR-γ agonist, which ameliorates insulin resistance, prevents hypertension and oxidative stress in rats with dietary-induced obesity [45]. It is possible that leptin, a polypeptide hormone mediator produced by adipocytes, stimulates oxidative stress generation in the brain [46]. In a previous study, we demonstrated that caloric restriction induces sympathoinhibition via reduction of oxidative stress in the RVLM of obesity-prone rats [20]. Although we did not determine the effects of insulin, leptin, or other adipocytokines on the AT_1R in the RVLM in the present study, we consider that peripheral adipose tissue might induce the activation of AT_1R-NAD (P) H oxidase–oxidative stress in the RVLM of obesity-induced hypertensive rats.

The obesity-induced hypertensive rats used in the present study have central obesity, impaired fasting glucose, low plasma adiponectin levels, hypertension, and sympathetic hyperactivity. These characteristics are consistent with those in previous studies using the same model [11,20], and with those observed in patients with MetS [1–4,6–8]. Furthermore, we demonstrated that either orally administered telmisartan or losartan has beneficial effects on the metabolic profile in obesity-induced hypertensive rats and that telmisartan has sympathoinhibitory effects. The findings of the present study suggest that ARBs are preferable for the treatment of hypertension in patients with MetS, consistent with previous studies [30,31]. Moreover, it is possible that orally administered telmisartan, but not losartan, inhibits SNS activity in patients with MetS.

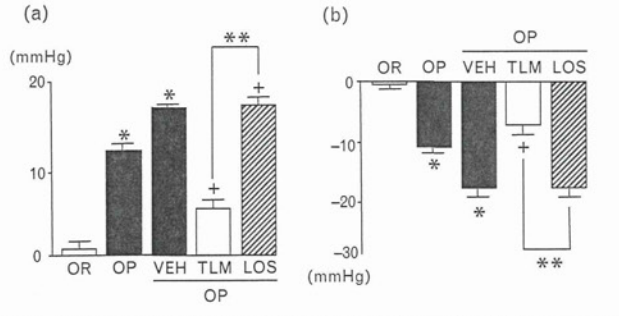

FIGURE 4 (a) Changes in mean arterial pressure caused by the microinjection of angiotensin II or (b) losartan into the bilateral rostral ventrolateral medulla of obesity-prone (OP) rats, obesity-resistant (OR) rats, telmisartan (TLM)-treated OP rats, losartan (LOS)-treated OP rats, and vehicle (VEH)-treated OP rats ($n = 5$ per group). *, $P < 0.05$ vs. OR in OP or VEH; +, $P < 0.05$ vs. VEH in TLM or LOS; **, $P < 0.05$ vs. TLM in LOS.

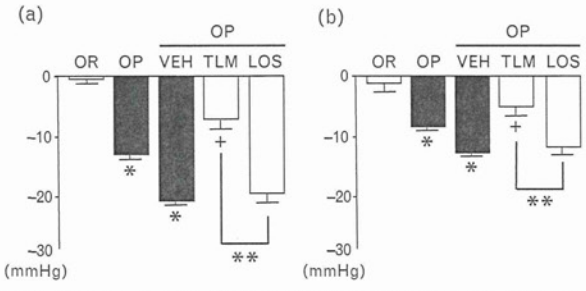

FIGURE 5 Changes in mean arterial pressure caused by the (a) microinjection of tempol or (b) apocynin into the bilateral rostral ventrolateral medulla of obesity-prone (OP) rats, obesity-resistant (OR) rats, telmisartan (TLM)-treated OP rats, losartan (LOS)-treated OP rats, and vehicle (VEH)-treated OP rats ($n = 5$ per group). *, $P < 0.05$ vs. OR in OP or VEH; +, $P < 0.05$ vs. VEH in TLM or LOS; **, $P < 0.05$ vs. TLM in LOS.

Further clinical studies are necessary to determine whether there are differences in the sympathoinhibitory effects among ARBs acting on the brain, particularly in the RVLM and hypothalamus.

In the present study, both telmisartan and losartan attenuated body weight gain during the course of treatment, whereas the daily calorie intake was not reduced. The results are consistent with previous studies in which ARBs improved energy expenditure and metabolic profiles in MetS [47–50]. It is possible that in MetS the ARB-induced attenuation of body weight gain and improvement of energy expenditure cause sympathoinhibition via a reduction of oxidative stress in the RVLM because we previously demonstrated that caloric restriction causes sympathoinhibition via a reduction of oxidative stress in the RVLM of obesity-prone rats [20]. The sympathoinhibition, however, was apparent in only the telmisartan-treated group and not in the losartan-treated group, despite their similar effects on body weight gain. Therefore, in the present study it is unlikely that the ARB-induced attenuation of body weight gain and the improvement of energy expenditure in obesity-prone rats were the main cause of the sympathoinhibition.

There are several limitations to the present study. First, we only examined oxidative stress in the RVLM. Several important nuclei are involved in cardiovascular control, such as the nucleus tractus solitarii and the hypothalamus. Reduction of SNS activity is also achieved by reducing AT_1R activity in the subfornical organ [51]. The increase in oxidative stress in obesity-induced hypertension and the reduction of oxidative stress by orally administered telmisartan may not be unique to the RVLM. In the regulation of SNS activity, however, the RVLM is the most important structure [9,10]. Furthermore, in the RVLM, oxidative stress is the most powerful and important sympathoexciting factor [12–14]. For these reasons, we focused on oxidative stress in the RVLM of obesity-induced hypertensive rats. Second, we cannot exclude the possibility that the benefits of telmisartan in the present study were due to its effects on the kidneys or vasculature. Third, in the present study, we measured blood pressure using the tail-cuff method and oxidative stress in the RVLM using the TBARS method and performed pharmacological examinations by acute microinjection of drugs into the RVLM in anesthetized rats after surgical preparations. Although it is preferable to measure blood pressure and heart rate using radiotelemetry, as in our previous studies [12–14,32], the 20-week observation period in the present study was too long for currently available radiotelemetry systems. Several methods are available for measuring oxidative stress in brain tissue, such as the dihydroethidium or lucigenin fluorescence methods, the electron spin resonance method, and the TBARS method. We previously demonstrated that the TBARS method is both reliable for measuring oxidative stress in the brain tissues and consistent with other methods [12], and we consider that the results obtained by the TBARS method provide a reliable parameter of oxidative stress in RVLM tissue. To inhibit NAD (P) H oxidase or superoxide production, we performed acute microinjection of tempol or apocynin into the RVLM in anesthetized rats. Moreover, we did not evaluate NAD (P) H oxidase isoforms in the present study, and, therefore, the precise mechanisms of NAD (P) H oxidase activation remain unclear. Chronic and awake procedures available by using gene transfer methods targeting AT_1R-NAD (P) H oxidase–oxidative stress in the RVLM locally would strengthen the present findings. Further studies are needed to investigate these issues.

In conclusion, orally administered telmisartan decreases SNS activity by inhibiting oxidative stress due to blockade of AT_1R-NAD (P) H oxidase in the RVLM of obesity-induced hypertensive rats. These results suggest that sympathoexcitation in obesity-induced hypertension is due to AT_1R-NAD (P) H oxidase–oxidative stress in the RVLM, and that orally administered telmisartan inhibits brain oxidative stress-induced sympathoexcitation in MetS through the blockade of AT_1R in the RVLM.

ACKNOWLEDGEMENTS

This study was supported by a Grant-in-Aid for Scientific Research from the Japan Society for the Promotion of Science (B193290231) and, in part, a Kimura Memorial Foundation Research Grant.

Conflicts of interest

There is no conflict of interest.

REFERENCES

1. Grundy SM, Cleeman JI, Daniels SR, Donato KA, Eckel RH, Franklin BA, *et al.* Diagnosis and management of the metabolic syndrome: an American Heart Association/National Heart, Lung, and Blood Institute Scientific Statement. *Circulation* 2005; 112:2735–2752.
2. Grundy SM. Metabolic syndrome pandemic. *Arterioscler Thromb Vasc Biol* 2008; 28:629–636.
3. Gami AS, Witt BJ, Howard DE, Erwin PJ, Gami LA, Somers VK, Montori VM. Metabolic syndrome and risk of incident cardiovascular events and death: a systematic review and meta-analysis of longitudinal studies. *J Am Coll Cardiol* 2007; 49:403–414.
4. Esler M, Straznicky N, Eikelis N, Masuo K, Lambert G, Lambert E. Mechanisms of sympathetic activation in obesity-related hypertension. *Hypertension* 2006; 48:787–796.
5. Raumouni K, Correla ML, Haynes WG, Mark AL. Obesity associated hypertension: new insights into mechanisms. *Hypertension* 2005; 45: 9–14.
6. Grassi G. Adrenergic overdrive as the link among hypertension, obesity, and impaired thermogenesis: lights and shadows. *Hypertension* 2007; 49:5–6.
7. Grassi G. Sympathetic overdrive and cardiovascular risk in the metabolic syndrome. *Hypertens Res* 2006; 29:839–847.
8. Landsberg L. Insulin-mediated sympathetic stimulation role in the pathogenesis of obesity-related hypertension (or, how insulin affects blood pressure, and why). *J Hypertens* 2001; 19:523–528.
9. Dampney RA. Functional organization of central pathways regulating the cardiovascular system. *Physiol Rev* 1994; 74:323–364.
10. Guyenet PG. The sympathetic control of blood pressure. *Nat Rev Neurosci* 2006; 7:335–346.
11. Stocker SD, Meador R, Adams JM. Neurons of the rostral ventrolateral medulla contribute to obesity-induced hypertension in rats. *Hypertension* 2007; 49:640–646.
12. Kishi T, Hirooka Y, Kimura Y, Ito K, Shimokawa H, Takeshita A. Increased reactive oxygen species in rostral ventrolateral medulla contribute to neural mechanisms of hypertension in stroke-prone spontaneously hypertensive rats. *Circulation* 2004; 109:3257–3262.
13. Kishi T, Hirooka Y, Konno S, Ogawa K, Sunagawa K. Angiotensin II type 1 receptor-activated caspase-3 through ras/mitogen-activated protein kinase/extracellular signal-regulated kinase in the rostral ventrolateral medulla is involved in sympathoexcitation in stroke-prone spontaneously hypertensive rats. *Hypertension* 2010; 55:291–297.
14. Hirooka Y, Sagara Y, Kishi T, Sunagawa K. Oxidative stress and central cardiovascular regulation. Pathogenesis of hypertension and therapeutic aspects. *Circ J* 2010; 74:827–835.

15. Dobrian AD, Davies MJ, Schriver SD, Lauterio TJ, Prewitt RL. Oxidative stress in a rat model of obesity-induced hypertension. *Hypertension* 2001; 37:554–560.
16. Smith AD, Brands MW, Wang MH, Dorrance AM. Obesity-induced hypertension develops in young rats independently of the renin-angiotensin-aldosterone system. *Exp Biol Med (Maywood)* 2006; 231:282–287.
17. Dandona P, Aljada A, Chaudhuri A, Mohanty P, Garg R. Metabolic syndrome: a comprehensive perspective based on interactions between obesity, diabetes, and inflammation. *Circulation* 2005; 111:1448–1454.
18. Zhang X, Dong X, Ren J, Driscoll MJ, Culver B. High dietary fat induces NADPH oxidase-associated oxidative stress and inflammation in rat cerebral cortex. *Exp Neurol* 2005; 191:318–325.
19. Nagae A, Fujita M, Kawarazaki H, Matsui H, Ando K, Fujita T. Sympathoexcitation by oxidative stress in the brain mediates arterial pressure elevation in obesity-induced hypertension. *Circulation* 2009; 119:978–986.
20. Kishi T, Hirooka Y, Ogawa K, Konno S, Sunagawa K. Calorie restriction inhibits sympathetic nerve activity via antioxidant effect in the rostral ventrolateral medulla of obesity-induced hypertensive rats. *Clin Exp Hypertens* 2011; 33:245–250.
21. Gao XY, Zhang F, Han Y, Wang HJ, Zhang Y, Guo R, Zhu GQ. AT1 receptor in rostral ventrolateral medulla mediating blunted baroreceptor reflex in spontaneously hypertensive rats. *Acta Pharmacol Sin* 2004; 25:1433–1438.
22. Koga Y, Hirooka Y, Araki S, Nozoe M, Kishi T, Sunagawa K. High salt intake enhances blood pressure increase during development of hypertension via oxidative stress in rostral ventrolateral medulla of spontaneously hypertensive rats. *Hypertens Res* 2008; 31:2075–2083.
23. Ito S, Komatsu K, Tsukamoto K, Kanmatsuse K, Sved AF. Ventrolateral medulla AT1 receptor support blood pressure in hypertensive rats. *Hypertension* 2002; 40:552–559.
24. Gohlke P, Weiss S, Jansen A, Wienen W, Stangier J, Rascher W, *et al.* AT1 receptor antagonist telmisartan administered peripherally inhibits central responses to angiotensin II in conscious rats. *J Pharmacol Exp Ther* 2001; 298:62–70.
25. Wang JM, Tan J, Leenen FHH. Central nervous system blockade by peripheral administration of AT1 receptor blockers. *J Cardiovasc Pharmacol* 2003; 41:593–599.
26. Lin Y, Matsumura K, Kagiyama S, Fukuhara M, Fujii K, Iida M. Chronic administration of olmesartan attenuates the exaggerated pressor response to glutamate in the lostral ventrolateral medulla of SHR. *Brain Res* 2005; 1058:161–166.
27. Lin Y, Tsuchihashi T, Kagiyama S, Matsumura K, Abe I. The influence of chronic antihypertensive treatment on the central pressor response in SHR. *Hypertens Res* 2001; 24:173–178.
28. Tsuchihashi T, Kagiyama S, Matsumura K, Abe I, Fujishima M. Effects of chronic oral treatment with imidapril and TCV-116 on the responsiveness to angiotensin II in ventrolateral medulla of SHR. *J Hypertens* 1999; 17:917–922.
29. Pelosch N, Hosomi N, Ueno M, Masugata H, Murao K, Hitomi H, *et al.* Systemic candesartan reduces brain angiotensin II via downregulation of brain renin-angiotensin system. *Hypertens Res* 2010; 33:161–164.
30. Elliott WJ, Meyer PM. Incident diabetes in clinical trials of antihypertensive drugs: a network meta-analysis. *Lancet* 2007; 369:201–207.
31. Ogihara T, Kikuchi K, Matsuoka H, Fujita T, Higaki J, Horiuchi M, *et al.*, Japanese Society of Hypertension Committee. The Japanese Society of Hypertension Guidelines for the Management of Hypertension (JSH 2009). *Hypertens Res* 2009; 32:3–107.
32. Nozoe M, Hirooka Y, Koga Y, Araki S, Konno S, Kishi T, *et al.* Mitochondria-derived reactive oxygen species mediate sympathoexcitation induced by angiotensin II in the rostral ventrolateral medulla. *J Hypertens* 2008; 26:2176–2184.
33. Benson SC, Pershadsingh HA, Ho CL, Chittinoyina A, Desai P, Pravanec M, *et al.* Identification of telmisartan as a unique angiotensin II receptor antagonist with selective PPARgamma-modulating activity. *Hypertension* 2004; 43:993–1002.
34. De Cavanagh EM, Felder LF, Felder MD, Stella IY, Toblli JE, Inserra F. Vascular structure and oxidative stress in salt-loaded spontaneously hypertensive rats: effects of losartan and atenolol. *Am J Hypertens* 2010; 23:1318–1325.
35. Marschall FH, Clark SA, Michel AD, Barnes JC. Binding of angiotensin antagonist to rat liver and brain membranes measured ex vivo. *Br J Pharmacol* 1993; 109:760–764.
36. Toyama K, Nakamura T, Kataoka K, Yasuda O, Fukuda M, Tokutomi Y, *et al.* Telmisartan protects against diabetic vascular complications in a mouse model of obesity and type 2 diabetes, partially through peroxisome proliferator activated receptor-γ-dependent activity. *Biochem Biophys Res Commun* 2011; 410:508–513.
37. Van Liefde I, Vauquelin G. Sartan-AT1 receptor interactions: in vitro evidence for insurmountable antagonism and inverse agonism. *Mol Cell Endocrinol* 2009; 302:237–243.
38. Yasuda N, Miura S, Akazawa H, Tanaka T, Qin Y, Kiya I, *et al.* Conformational switch of angiotensin II type 1 receptor underlying mechanical stress-induced activation. *EMBO Rep* 2008; 9:179–186.
39. Miura S, Karnik SS, Saku K. Review: angiotensin II type 1 receptor blockers: class effects versus molecular effects. *J Renin Angiotensin Aldosterone Syst* 2011; 12:1–7.
40. Chan SH, Wu KL, Kung PS, Chan JY. Oral intake of rosiglitazone promotes a central antihypertensive effect via upregulation of peroxisome proliferator-activated receptor-gamma and alleviation of oxidative stress in rostral ventrolateral medulla of spontaneously hypertensive rats. *Hypertension* 2010; 55:1444–1453.
41. Schupp M, Janke J, Clasen R, Unger T, Kintscher U. Angiotensin type I receptor blockers induce peroxisome proliferator-activated receptor-γ activity. *Circulation* 2004; 109:2054–2057.
42. Zimmerman MC, Lazartigues E, Sharma RV, Davisson RL. Hypertension caused by angiotensin II infusion involves increased superoxide production in the central nervous system. *Circ Res* 2004; 95:210–216.
43. Zimmerman MC, Lazartigues E, Lang JA, Sinnayah P, Ahmad IM, Spitz DR, Davisson RL. Superoxide mediates the actions of angiotensin II in the central nervous system. *Circ Res* 2002; 91:1038–1045.
44. Boustany CM, Bharadwaj K, Daugherty A, Brown DR, Randall DC, Cassis LA. Activation of the systemic and adipose renin-angiotensin system in rats with diet-induced obesity and hypertension. *Am J Physiol* 2004; 287:R943–R949.
45. Dobrian AD, Schriver SD, Khraibi AA, Prewitt RL. Pioglitazone prevents hypertension and reduces oxidative stress in diet-induced obesity. *Hypertension* 2004; 43:48–56.
46. Lauterio TJ, Davies MJ, DeAngelo M, Peyser M, Lee J. Neuropeptide Y expression and endogenous leptin concentrations in a dietary model of obesity. *Obes Res* 1999; 7:498–505.
47. Basso N, Cini R, Pietrelli A, Ferder L, Terragno NA, Inserra F. Protective effect of long-term angiotensin II inhibition. *Am J Physiol* 2007; 293:H1351–H1358.
48. Kamari Y, Harari A, Shaish A, Peleg E, Sharabi Y, Harats D, Grossman E. Effect of telmisartan, angiotensin II receptor antagonist, on metabolic profile in fructose-induced hypertensive, hyperinsulinemic, hyperlipidemic rats. *Hypertens Res* 2008; 31:135–140.
49. Khan AH, Lmig JD. Telmisartan provides better renal protection than valsartan in a rat model of metabolic syndrome. *Am J Hypertens* 2011; 24:816–821.
50. Kouyama R, Suganami T, Nishida J, Tanaka M, Toyoda T, Kiso M, *et al.* Attenuation of diet-induced wight gain and adiposity through increased energy expenditure in mice lacking angiotensin II type 1a receptor. *Endocrinology* 2005; 146:3481–3489.
51. Benicky J, Sanchez-Lemus E, Honda M, Pang T, Orecna M, Wang J, *et al.* Angiotensin II AT1 receptor blockade ameliorates brain inflammation. *Neuropsychopharmacology* 2011; 36:857–870.

Reviewers' Summary Evaluations

Referee 1

The main strength of this paper is the finding that oxidative stress in the brainstem can be modulated pharmacologically, with a generally very safe class of drugs, to reduce sympathetic activity and improve metabolic control in experimental obesity. The main limitation is that the explanation for the superiority of telmisartan over losartan (and presumably other angiotensin receptor blockers) in reducing oxidative stress is not securely established.

Referee 2

Chronic oral administration of telmisartan reduces sympathetic activity to a greater extent than losartan in obesity-prone rats while both drugs reduce arterial pressure by a similar magnitude. The differential effects on sympathetic activity are at least in part due to a higher potency of telmisartan to block AT1 receptors and to inhibit superoxide formation in the RVLM. It remains open if reduced sympathetic activity in telmisartan-treated rats results in less organ damage and better survival. Furthermore, localization and enzymatic sources of elevated superoxide formation within the RVLM of obesity-prone rats remain to be more clearly identified.

Nanoparticle-Mediated Delivery of Pioglitazone Enhances Therapeutic Neovascularization in a Murine Model of Hindlimb Ischemia

Ryoji Nagahama, Tetsuya Matoba, Kaku Nakano, Shokei Kim-Mitsuyama, Kenji Sunagawa, Kensuke Egashira

Objective—Critical limb ischemia is a severe form of peripheral artery disease (PAD) for which neither surgical revascularization nor endovascular therapy nor current medicinal therapy has sufficient therapeutic effects. Peroxisome proliferator activated receptor-γ agonists present angiogenic activity in vitro; however, systemic administration of peroxisome proliferator–activated receptor-γ agonists is hampered by its side effects, including heart failure. Here, we demonstrate that the nanoparticle (NP)-mediated delivery of the peroxisome proliferator activated receptor-γ agonist pioglitazone enhances its therapeutic efficacy on ischemia-induced neovascularization in a murine model.

Methods and Results—In a nondiabetic murine model of hindlimb ischemia, a single intramuscular injection of pioglitazone-incorporated NP (1 μg/kg) into ischemic muscles significantly improved the blood flow recovery in the ischemic limbs, significantly increasing the number of CD31-positive capillaries and α-smooth muscle actin–positive arterioles. The therapeutic effects of pioglitazone-incorporated NP were diminished by the peroxisome proliferator activated receptor-γ antagonist GW9662 and were not observed in endothelial NO synthase–deficient mice. Pioglitazone-incorporated NP induced endothelial NO synthase phosphorylation, as demonstrated by Western blot analysis, as well as expression of multiple angiogenic growth factors in vivo, including vascular endothelial growth factor-A, vascular endothelial growth factor-B, and fibroblast growth factor-1, as demonstrated by real-time polymerase chain reaction. Intramuscular injection of pioglitazone (1 μg/kg) was ineffective, and oral administration necessitated a >500 μg/kg per day dose to produce therapeutic effects equivalent to those of pioglitazone-incorporated NP.

Conclusion—NP-mediated drug delivery is a novel modality that may enhance the effectiveness of therapeutic neovascularization, surpassing the effectiveness of current treatments for peripheral artery disease with critical limb ischemia. ***(Arterioscler Thromb Vasc Biol.* 2012;32:2427-2434.)**

Key Words: endothelium ■ nitric oxide synthase ■ peripheral arterial disease ■ nanoparticle ■ pioglitazone

Peripheral artery disease (PAD) is a common disorder that causes claudication, ischemic pain, and ulcers in the lower extremities and that often requires limb amputation when it develops into critical limb ischemia (CLI). Currently, there is no effective medicinal therapy for CLI. The standard therapy for CLI is lower-extremity revascularization, either by bypass surgery or by endovascular therapy, or lower limb amputation, which is associated with a poor prognosis when revascularization is not applicable. Surgical revascularization is associated with ≈5% perioperative mortality rate and a complication rate of 30% to 50%.[1,2] Endovascular therapy is an option for selected patients with CLI; however, this therapy is rarely an option and is associated with inferior patency. Hence, there is an unmet need for less invasive medical therapies to improve the quality of life and prognosis of patients with peripheral artery disease.

See accompanying article on page 2337

The peroxisome proliferator activated receptor-γ (PPAR-γ) agonists thiazolidines (TZDs) are in clinical use for treating type 2 diabetes mellitus to improve insulin sensitivity in skeletal muscles. PPAR-γ is also expressed in vascular cells, and the TZDs troglitazone and pioglitazone stimulate the migration, proliferation, and survival of endothelial cells and endothelial progenitor cells via the expression of growth factors and cytokines in vitro.[3,4] This effect suggests that TZDs may enhance ischemic neovascularization. By contrast, the high-dose TZDs troglitazone and rosiglitazone suppress vascular endothelial growth factor (VEGF)–induced

Received on: June 6, 2012; final version accepted on: July 25, 2012.

From the Department of Cardiovascular Medicine, Graduate School of Medical Sciences, Kyushu University, Fukuoka, Japan (R.N., T.M., K.S.); Department of Cardiovascular Research, Development, and Translational Medicine, Kyushu University Graduate School of Medical Sciences, Fukuoka, Japan (K.N., K.E.); and Department of Pharmacology and Molecular Therapeutics, Faculty of Life Sciences, Kumamoto University, Kumamoto, Japan (S.K.-M.).

The online-only Data Supplement is available with this article at http://atvb.ahajournals.org/lookup/suppl/doi:10.1161/ATVBAHA.112.253823/-/DC1.

Correspondence to Tetsuya Matoba, MD, PhD, Department of Cardiovascular Medicine, Kyushu University Graduate School of Medical Sciences, 3-1-1, Maidashi, Higashi-ku, Fukuoka 812–8582, Japan. E-mail matoba@cardiol.med.kyushu-u.ac.jp

endothelial cell proliferation via suppressing VEGF receptor 1 (Flt-1) and 2 (Flk/KDR) expression in vitro.[5] Likewise, there are controversial reports regarding in vivo neovascularization using different TZDs in different models.[6–8] Pioglitazone exerts therapeutic angiogenesis in vivo in hindlimb ischemia in a murine model;[9] however, it remains unclear whether pioglitazone-induced angiogenesis depends solely on PPAR-γ activation in endothelial cells or whether it depends on the improvement of hyperglycemia.

Despite its potential therapeutic effect on ischemic neovascularization, the systemic administration of pioglitazone is hampered by its undesirable side effects, including edema and heart failure, which may be optimized by a novel drug delivery system. Recently, we reported that polylactic–glycolic acid (PLGA) nanoparticles (NP) accumulate in the capillary and arteriolar endothelium after intramuscular injection in murine[10] and rabbit[11] models of hindlimb ischemia. The application of PLGA NP as a drug delivery system for pioglitazone may enhance its therapeutic efficacy and may reduce the possible side effects. In this study, we tested our hypothesis that pioglitazone induces therapeutic neovascularization in a nondiabetic murine model of hindlimb ischemia and that the NP-mediated delivery of pioglitazone enhances the therapeutic efficacy of pioglitazone.

Materials and Methods

Preparation of PLGA NP

We prepared PLGA NP incorporating pioglitazone (Pio-NP; Takeda Pharmaceutical Company Limited, Osaka, Japan) or fluorescein isothiocyanate (FITC) (FITC-NP) via the emulsion solvent diffusion method.[12] PLGA was quickly dissolved in a mixture of acetone and methanol, and pioglitazone or FITC was then added. The resultant polymer-FITC or polymer-pioglitazone solution was emulsified in polyvinyl alcohol solution under stirring at 400 rpm using a propeller-type agitator with 3 blades (Heidon 600G; Shinto Scientific, Japan). After agitating the system for 2 hours under reduced pressure at 40°C, the entire suspension was centrifuged (20 000*g* for 20 minutes at −20°C). After removing the supernatant, purified water was mixed with the sediment. The wet mixture was then centrifuged again to remove the excess polyvinyl alcohol and the unencapsulated reagent that could not be adsorbed by the surfaces of NP. After repeating this process, the resultant dispersion was freeze-dried under the same conditions. The FITC-NP was 4.2% (wt/vol) FITC and Pio-NP was 3.7% (wt/vol) pioglitazone.

Animal Preparation and Experimental Protocol

The study protocol was reviewed and approved by the Committee on Ethics on Animal Experiments, Kyushu University Faculty of Medicine, and the experiments were conducted according to the Guidelines of the American Physiological Society. All mice were maintained in the Laboratory of Animal Experiments at Kyushu University. After anesthesia with an intraperitoneal injection of ketamine hydrochloride (70 mg/kg) and xyladine hydrochloride (3 mg/kg), we induced unilateral hindlimb ischemia in the mice by ligation and excision of the femoral arteries and veins, as previously described.[10] Immediately after inducing ischemia, the animals were divided into treatment groups and were euthanized on day 21. Hindlimb blood flow measurements were performed using a laser Doppler perfusion imaging (LDPI) analyzer (Moor Instruments, United Kingdom). The LDPI index was expressed as the ratio of the LDPI signal in the ischemic limb compared with that in the normal limb. In protocols 1, 2, and 3, the animals received an intramuscular injection of therapeutic agents into the left femoral and thigh muscles using a 27-gauge needle immediately after inducing ischemia, as indicated (Methods and Figure I in the online-only Data Supplement). In protocol 4, the animals received a daily oral treatment of pioglitazone or vehicle (Methods and Figure I in the online-only Data Supplement).

Distribution of FITC-NP in Ischemic Hindlimb Tissues

Three, 7, 14, and 21 days after hindlimb ischemia and intramuscular injection of FITC-NP, the gastrocnemius muscle was isolated from ischemic and nonischemic limbs, and the FITC signals were examined under a fluorescent microscope. Frozen cross sections of the muscles 3 days after hindlimb ischemia and intramuscular injection of FITC or FITC-NP were then prepared and examined under a fluorescent microscope (Biozero; Keyence, Co, Osaka, Japan). The nuclei were counterstained with 4′,6-diamidino-2-phenylindole (DAPI; Vector Shield, Vector Labs Ltd, United Kingdom) in some sections. Other sections were stained with anti-mouse platelet/endothelial cell adhesion molecule-1 antibody (CD31; Santa Cruz Biotechnology, Inc, Santa Cruz, CA) as the primary antibody and anti-goat IgG (Alexa 555; Life Technologies, Grand Island, NY) as the secondary antibody.

Histological and Immunohistochemical Analyses

A histological and immunohistochemical evaluation was performed in 5-μm paraffin-embedded sections of the gastrocnemius muscle after hindlimb ischemia. To determine the capillary and arteriolar density, cross sections were stained with anti-mouse platelet endothelial cell adhesion molecule with anti–platelet/endothelial cell adhesion molecule-1 (CD31) antibody as a primary antibody (Santa Cruz Biotechnology, Inc) and anti-goat IgG antibody (Alexa 555; Life Technologies) as a secondary antibody. The nuclei were counterstained with DAPI (Vector Laboratories, Inc, Burlingame, CA) and α-smooth muscle actin antibody (DAKO, Glostrup, Denmark).

Measurements of Pioglitazone Concentration in the Serum and Muscle Tissue

The pioglitazone concentrations in the serum and the muscle were measured at predetermined time points using liquid chromatography coupled to tandem mass spectrometry. Additional details are provided in the Methods in the online-only Data Supplement.

PPAR-γ Activity Measurement in the Muscle Tissue

Nuclear extracts were prepared from the gastrocnemial muscle homogenates using a nuclear extract kit (NE-PER Nuclear and Cytoplasmic Extraction Reagents; Thermo Fisher Scientific Inc, Rockford, IL) according to the manufacturer's instructions. The protein was measured using a BCA Protein Assay kit (Thermo Fisher Scientific Inc). PPAR-γ activation was assayed using ELISA-based PPAR-γ activation TransAM kit (Active Motif, Rixensart, Belgium), which was used according to the manufacturer's instructions. Ten micrograms of nuclear protein samples were incubated for 1 hour in a 96-well plate coated with an oligonucleotide that contains a PPAR response element domain (5′-AACTAGGTCAAAGGTCA-3′), to which the activated PPAR-γ contained in nuclear extracts specifically binds. After washing, PPAR-γ antibody (1:1000 dilutions) was added to these wells and incubated for 1 hour. After incubation for 1 hour with a secondary horseradish peroxidase–conjugated antibody (1:1000 dilution), specific binding was detected by colorimetric estimation at 450 nm with a reference wavelength of 655 nm.

Polymerase Chain Reaction Array

The total RNA was isolated from the gastrocnemial muscles using an RNeasy Fibrous Tissue Mini kit (QIAGEN Inc, Valencia, CA). cDNA synthesis was performed using 1 μg of the total RNA with a PrimeScript RT reagent kit (Takara-Bio, Inc, Shiga, Japan). For angiogenic factor expression analysis, quantitative real-time polymerase chain reaction analysis of 84 angiogenic factors was performed using mouse-specific angiogenic factors RT2 Profiler PCR Arrays (QIAGEN Inc),

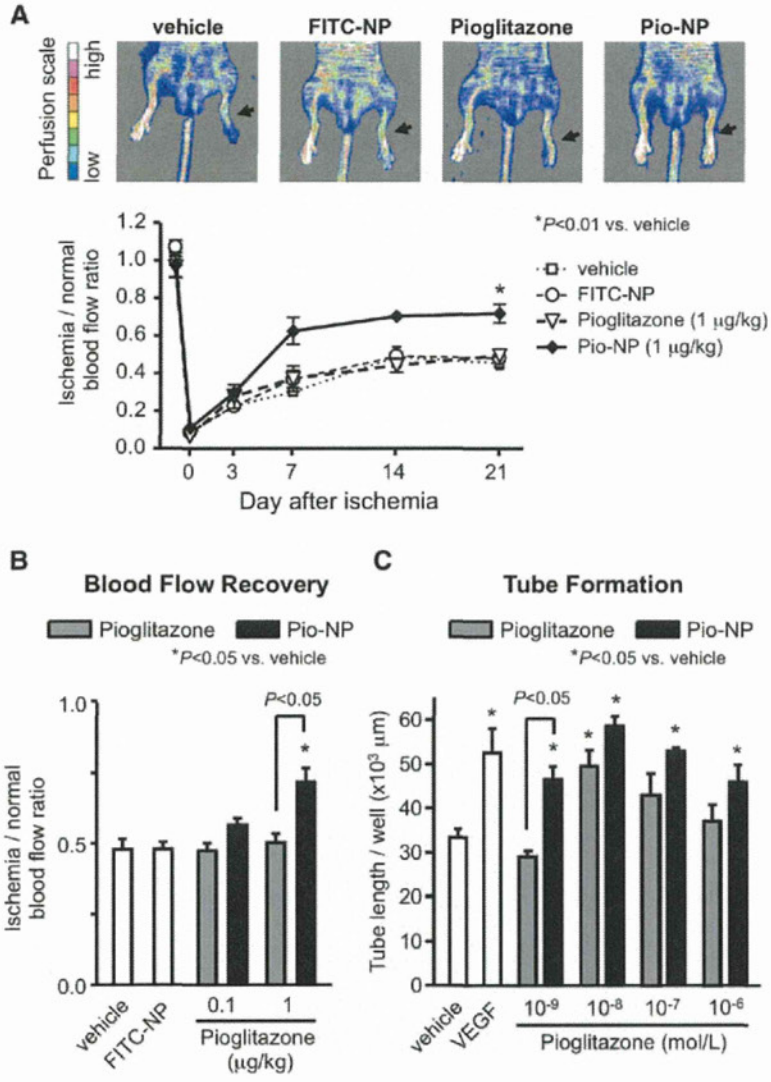

Figure 1. The effects of pioglitazone and pioglitazone-incorporated nanoparticle (Pio-NP) on ischemia-induced neovascularization. **A**, Representative laser Doppler perfusion imaging (LDPI) 21 days after inducing hindlimb ischemia (upper images). The arrow indicates ischemic limb. Quantification of LDPI-derived blood flow recovery. n=6 to 7. *P<0.01 vs no treatment group. The data were compared using 1-way ANOVA followed by Bonferroni multiple comparison tests. **B**, Quantification of LDPI-derived blood flow recovery 21 days after induction of hindlimb ischemia. n=6 to 7. The data were compared using 2-way ANOVA followed by Bonferroni multiple comparison tests. *P<0.05 vs control. **C**, The effects of Pio-NP or pioglitazone on the angiogenic capacity of human endothelial cells in vitro. Quantitative analysis of tube formation (tube length) of 4 independent experiments. The data were compared using 2-way ANOVA followed by Bonferroni multiple comparison tests. *P<0.05 vs control. VEGF indicates vascular endothelial growth factor; FITC, fluorescein isothiocyanate.

according to the manufacturer's protocol. The complete list of the genes analyzed is available online at http://www.sabiosciences.com/rt_pcr_product/HTML/PARN-030A.html. The relative gene expression levels were normalized to the housekeeping gene hypoxanthine phosphoribosyltransferase-1. Data analysis was performed using the ΔΔCt-based fold-change method.

Angiogenesis Assay in Human Umbilical Vein Endothelial Cells

We performed a 2-dimensional Matrigel assay in human umbilical vein endothelial cells. Additional details are provided in the Methods in the online-only Data Supplement.

Western Blot Analysis

The homogenates of the muscle tissues were analyzed for immunoblotting 3 days after inducing hindlimb ischemia. The membrane was incubated with antibodies against phosphorylated Akt, phosphorylated endothelial NO synthase (eNOS), Akt (Cell Signaling, Danvers, MA), and eNOS (Thermo Fisher Scientific Inc).

Statistical Analysis

The data are expressed as the mean±SEM. The statistical analysis was assessed using analysis of variance and multiple comparison tests. P values <0.05 were considered to be statistically significant.

Results

Tissue Distribution of PLGA NP

We first examined the distribution of FITC after an injection of either FITC-NP or FITC into ischemic hindlimb muscles in a murine model. FITC fluorescence was detectable for 14 days in the FITC-NP–injected hindlimbs, whereas FITC fluorescence was undetectable at day 7 in FITC only–injected hindlimbs (Figure II in the online-only Data Supplement), suggesting NP-dependent modification of pharmacokinetics as shown in our previous study.[10]

Pio-NP Enhanced Ischemia-Induced Neovascularization

We examined the effect of Pio-NP on blood flow recovery after induction of acute hindlimb ischemia in a murine model using LDPI. Importantly, a single intramuscular injection of Pio-NP containing 1 μg/kg pioglitazone significantly enhanced blood flow recovery in the ischemic limbs, whereas an intramuscular injection of PBS (vehicle), FITC-NP, or 1 μg/kg pioglitazone had no therapeutic effects (Figure 1A and 1B). After injecting pioglitazone or Pio-NP into ischemic hindlimbs, we examined the tissue and serum concentration of pioglitazone at several

Table 1. Tissue and Serum Pioglitazone Concentrations After Intramuscular Injection of Pioglitazone or Pioglitazone-NP

	Time After Injection			
	15 min	1 h	6 h	24 h
Pioglitazone only at 1 μg/kg				
Muscle, ng/g tissue	19±1	ND	ND	ND
Serum, ng/mL	1±1	ND	1±1	ND
Pioglitazone-NP containing 1 μg/kg pioglitazone				
Muscle, ng/g tissue	37±4*	5±2	2±1	ND
Serum, ng/mL	2±1	1±1	2±0	ND

ND indicates not detected (muscle <1 ng/g tissue; serum <1 ng/mL); NP, nanoparticle.

*$P<0.05$ vs pioglitazone.

time points. As shown in Table 1, Pio-NP remained detectable for 6 hours in the muscular tissue compared with pioglitazone alone. The concentration of pioglitazone in the muscular tissue was estimated to be 37±4 ng/g tissue 15 minutes after injecting Pio-NP containing 1 μg/kg pioglitazone and was below the detectable limit (≈1.0 ng/g tissue) after 24 hours. By contrast, pioglitazone was undetectable 1 hour after injecting 1 μg/kg pioglitazone alone (Table 1), suggesting that NP enhanced the accumulation of pioglitazone within the hindlimb tissue.

We then tested the angiogenic activity of pioglitazone in cultured endothelial cells in vitro. Pio-NP induced significant endothelial tube formation in human umbilical vein endothelial cells at 10^{-9} to 10^{-6} mol/L, which was equivalent to the effect induced by VEGF (10 ng/mL; Figure 1C). The induction of endothelial tube formation was significantly enhanced with Pio-NP compared with pioglitazone alone at the same doses, suggesting that NP modified the drug kinetics and efficacy. Pio-NP–induced blood flow recovery was accompanied by a significant increase in the number of CD31-positive endothelial cells surrounding the regenerating myocytes and an increase in number of capillary and arterioles accompanied by α-smooth muscle actin–positive smooth muscle cells 21 days after inducing ischemia (Figure 2).

Pio-NP Enhances Ischemic Neovascularization Through PPAR-γ Activation

We questioned whether Pio-NP–induced neovascularization is dependent solely on PPAR-γ activation. The blood flow recovery by Pio-NP was reversed in mice pretreated with the PPAR-γ antagonist GW9662, suggesting that PPAR-γ activation is critical for Pio-NP–induced blood flow recovery (Figure 3A). Indeed, Pio-NP significantly activated PPAR-γ DNA binding in the nuclear extract from the ischemic hindlimb tissues. Systemic pretreatment with GW9662 again reversed the Pio-NP–induced PPAR-γ activation in the hindlimb tissues (Figure 3B, left). By contrast, an intramuscular injection of Pio-NP in the ischemic limbs did not affect PPAR-γ transcriptional activity in the contralateral nonischemic limbs (Figure 3B, right). The serum levels of glucose, triglyceride, and insulin did not differ between the control group and the oral administration of pioglitazone groups. This result suggests that pioglitazone enhances ischemic neovascularization independent of blood glucose or insulin, even when administered daily, in the nondiabetic murine model (Table I in the online-only Data Supplement).

Effect of Pio-NP on Endogenous Angiogenic Factor Expression

PPAR-γ may regulate several genes that contribute to ischemic neovascularization. Three days after inducing ischemia, we examined gene expression in the hindlimb tissues that were treated with Pio-NP. Real-time polymerase chain reaction analysis revealed a significant induction of VEGF-A, VEGF-B, VEGF receptor1/Flt-1, fibroblast growth factor-1 (FGF-1), FGF receptor 3, and platelet/endothelial cell adhesion molecule-1 in the ischemic muscle tissues treated with Pio-NP compared with vehicle-treated ischemic muscle tissues (Table 2).

Effects of Pio-NP on Neovascularization Depends on eNOS

The aforementioned angiogenic growth factors were demonstrated to induce the proliferation of endothelial cells, in

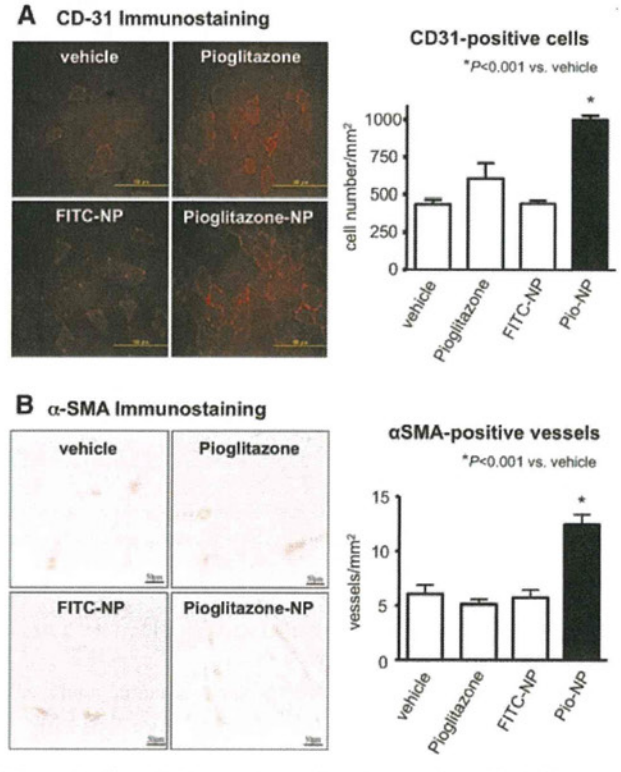

Figure 2. Quantitative analysis of angiogenesis and arteriogenesis. **A**, Immunofluorescent staining of cross sections from ischemic muscle at 21 days after inducing ischemia, stained for the endothelial marker CD31 (red; left). Scale bars, 100 μm. Quantitative analysis of angiogenesis (right; CD31-positive cells per mm²). **B**, Representative micrographs of ischemic muscle sections stained immunohistochemically with antibodies against α-smooth muscle actin (α-SMA) at 21 days after surgery (left). The nuclei were counterstained with hematoxylin. Scale bars, 100 μm. Quantitative analysis of arteriogenesis (right; α-SMA–positive vessels per mm²). The data were compared using 1-way ANOVA followed by Bonferroni multiple comparison tests. *$P<0.001$ vs untreated group. Pio-NP indicates pioglitazone-incorporated nanoparticle.

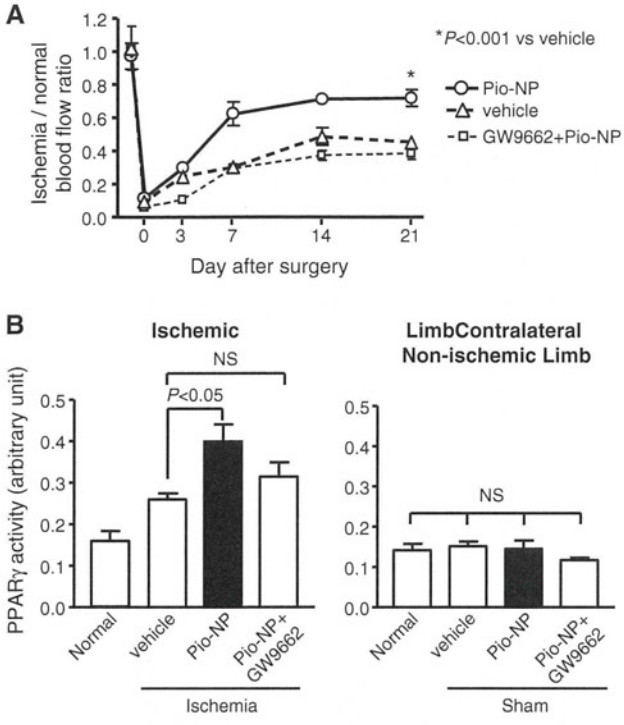

Figure 3. The essential role of peroxisome proliferator–activated receptor-γ (PPAR-γ) in the enhanced ischemia-induced neovascularization induced by pioglitazone-incorporated nanoparticle (Pio-NP). The increased neovascularization induced by Pio-NP was associated with PPAR-γ activity. **A**, Quantification of laser Doppler–derived blood flow recovery after surgery in wild-type mice with or without administration of GW9662, a PPAR-γ inhibitor. **B**, PPAR-γ activation in ischemic muscles 3 days after ischemia. The data were compared using 1-way ANOVA followed by Bonferroni multiple comparison tests. NS indicates not significant.

which endothelial NO plays a critical role.[13] PPAR-γ activation induces NO release from endothelial cells, both dependently and independently of eNOS mRNA expression.[14,15] Hence, we examined the role of eNOS expression and its activation in Pio-NP–induced neovascularization in the ischemic hindlimb model. In $eNOS^{-/-}$ mice, femoral artery occlusion induced a relatively severe lesion compared with wild-type mice (data not shown), whereas blood flow recovery determined by LDPI was equivalent in untreated $eNOS^{-/-}$ mice compared with wild-type mice. Importantly, the Pio-NP–induced enhancement was not observed in $eNOS^{-/-}$ mice (Figure 4A), suggesting the critical role of eNOS in the therapeutic effects of Pio-NP. Pio-NP did not affect eNOS mRNA expression (data not shown) and the eNOS protein levels in the ischemic hindlimb tissues in wild-type mice (Figure 4B and 4C). The treatment with Pio-NP significantly increased the phosphorylation of eNOS in ischemic muscles compared with nonischemic control and nontreated ischemic muscles 3 days after treatment (Figure 4C). Pio-NP tended to increase Akt phosphorylation compared with no treatment, although the difference was not statistically significant.

Efficacy of the PLGA NP

Finally, we confirmed the therapeutic advantage of the NP-mediated intramuscular delivery of pioglitazone over pioglitazone alone or the oral administration of pioglitazone. The daily oral administration of pioglitazone (1 μg/kg per day) did not enhance blood flow recovery. Oral treatment with pioglitazone required as high as 1000 μg/kg per day to significantly enhance blood flow recovery equivalent to Pio-NP (Figure 5A). Finally, a single intramuscular injection of Pio-NP was significantly more effective compared with a single intramuscular injection of pioglitazone alone or daily oral administration of pioglitazone at the same single dose (1 μg/kg) (Figure 5B).

Table 2. Gene Expression Changes in Pioglitazone-Incorporated Nanoparticle–Treated Ischemic Muscle Tissue Compared With Vehicle-Treated Tissue (Real-Time Polymerase Chain Reaction Array)

Gene Name	Description	Epox/Control Normalized (Increase)	Reference Sequence
FGF-6	Fibroblast growth factor-6	6.04	NM_010204
VEGF-B	Vascular endothelial growth factor-B	3.39	NM_011697
FGF-1	Fibroblast growth factor-1	3.06	NM_010197
—	T-box–1	2.86	NM_011532
PECAM-1	Platelet/endothelial cell adhesion molecule-1	2.61	NM_008816
Agpt2	Angiopoietin-2	2.56	NM_007426
VEGF-A	Vascular endothelial growth factor-A	2.26	NM_009505
EGF	Epidermal growth factor	2.06	NM_010113
Galpha13/ AU024132	Guanine nucleotide binding protein, α13	1.96	NM_010303
VEGFR-1/Flt-1	Vascular endothelial growth factor receptor 1	1.90	NM_010228
FGFR-3	Fibroblast growth factor receptor-3	1.74	NM_008010
VEGF-D	Vascular endothelial growth factor-D	1.74	NM_010216

Gene Name	Description	Epox/Control Normalized (Decrease)	Reference Sequence
MK/Mek	Midkine	2.14	NM_010784
TGF-β1	Transforming growth factor-β1	1.78	NM_011577
CINC-2a/Gro2/ MIP-2//Mgsa-b/ Scyb2	Chemokine (C-X-C motif) ligand-2	1.62	NM_009140
ELF-2/Htk-L/ LERK-5	Ephrin-B2	1.60	NM_010111
TSP2/Thbs-2	Thrombospondin-2	1.52	NM_011581

Discussion

There have been controversial results regarding the angiogenic effects of TZDs both in vitro and in vivo.[16] In the present study, we demonstrated that oral treatment with pioglitazone at clinically relevant dose (1000 μg/kg) enhanced blood flow recovery in a hindlimb ischemia model in nondiabetic mice independent of the changes in blood glucose

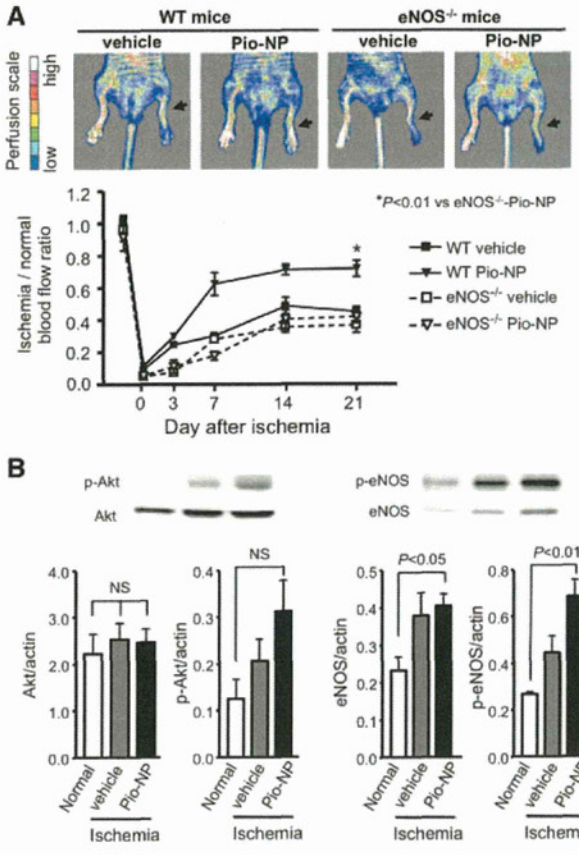

Figure 4. The essential role of endothelial nitric oxide synthase (eNOS) in the enhanced ischemia–induced neovascularization induced by pioglitazone-incorporated nanoparticle (Pio-NP). The increased neovascularization by the Pio-NP was associated with the increased expression of the active forms of eNOS and Akt. **A**, Quantification of laser Doppler–derived blood flow recovery after surgery in wild-type (WT) mice and in eNOS$^{-/-}$ mice. n=5 to 6. *P<0.01 vs no treatment group. **B**, Western blot analysis of phosphorylated Akt and eNOS in ischemic and nonischemic muscles 3 days after ischemia. The quantitative evaluation was expressed as a ratio of phosphorylated Akt, phosphorylated eNOS (p-eNOS), Akt, eNOS to actin. n=4 to 6. The data were compared using 1-way ANOVA followed by Bonferroni multiple comparison tests. NS indicates not significant.

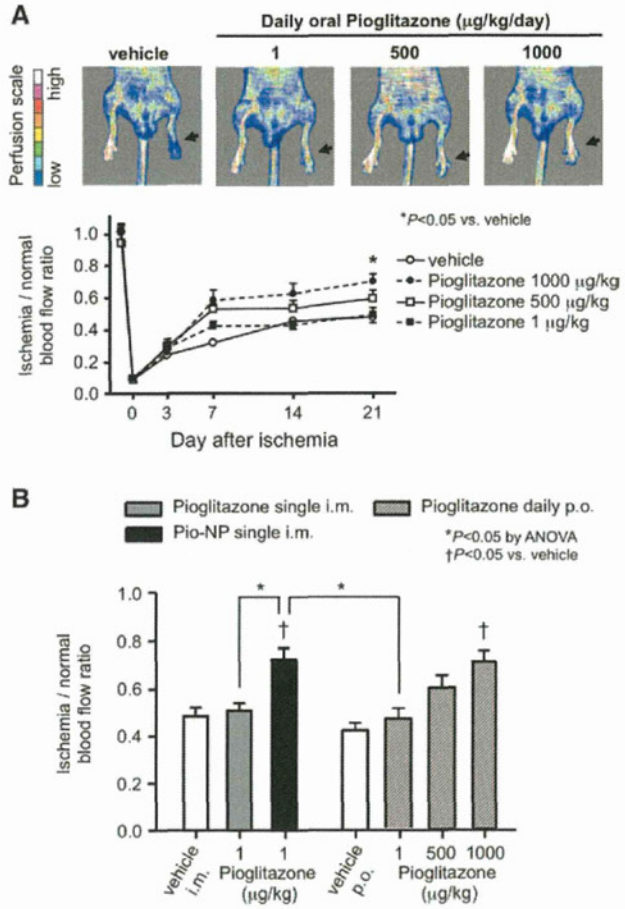

Figure 5. Effects of the daily oral administration of pioglitazone on ischemia-induced neovascularization. **A**, Quantification of laser Doppler perfusion imaging (LDPI)–derived blood flow recovery. n=7 to 8. *P<0.01 vs untreated group. **B**, The effects of single intramuscular injection of pioglitazone- incorporated nanoparticle (Pio-NP) compared with the daily oral administration of pioglitazone 21 days after ischemia. n=7 to 8.

or insulin levels, suggesting that pioglitazone directly acts on vascular cells to enhance ischemia-induced neovascularization. Despite its potential effectiveness, the oral administration of pioglitazone is hampered by its adverse effects, including edema and heart failure.[17] Recently, the potential link between pioglitazone and the risk of bladder cancer has been raised as a concern.[18]

Importantly, we demonstrated that a single intramuscular injection of Pio-NP at as low a concentration as 1 μg/kg had significant therapeutic effects on ischemia-induced neovascularization (Figure 1). The pioglitazone concentrations in the tissue and the serum suggest the local retention of Pio-NP in ischemic skeletal muscles in vivo. The distribution of FITC-NP (Figure II in the online-only Data Supplement) suggests that Pio-NP accumulates in the endothelial cells in the ischemic muscles. In our previous studies,[10,11] we have shown that PLGA NP accumulates preferentially in endothelial cells compared with skeletal muscle cells, relying on clathrin-mediated endocytosis, which may explain the selective distribution in endothelial cells in the muscle tissues. A single intramuscular injection of PLGA NP may cover the therapeutic window for the blood flow recovery in the murine model (≈7 days; eg, Figure 1A), given that we have also demonstrated that PLGA NP (mean diameter =200 nm) gradually undergo hydrolysis over 21 days in a physiological fluid (pH 7.4; 32°C).[10] Importantly, Pio-NP exhibited a significant induction of endothelial tube formation at a wider range of doses (10^{-9} to 10^{-6} mol/L) compared with pioglitazone alone (Figure 1C), suggesting that PLGA NP–dependent changes in tissue distribution and release kinetics optimized the proangiogenic activity of pioglitazone on endothelial cells. Further studies are needed to clarify the effect of ischemia and the amount of PLGA NP on the mode of endosomal escape, intracellular localization, and drug release kinetics of PLGA NP used in the present study.[19]

PPAR-γ activation appears to be a critical step in therapeutic neovascularization by Pio-NP because we confirmed that Pio-NP induced PPAR-γ DNA binding to the PPAR response element (Figure 3B) and that the PPAR-γ antagonist GW9662 abolished the blood flow recovery by Pio-NP (Figure 3A).

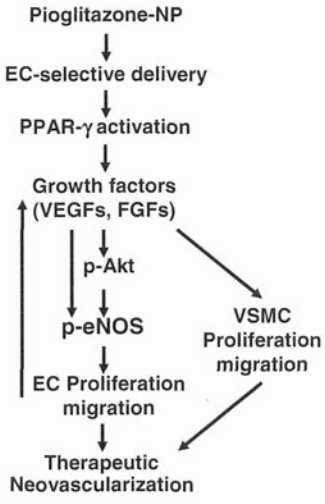

Figure 6. Schematic illustration of the effects of pioglitazone nanoparticles. The nanoparticle (NP)–mediated endothelial cell–selective delivery of pioglitazone induces peroxisome proliferator activated receptor-γ (PPAR-γ) activation. PPAR-γ activation with pioglitazone enhances the expression of multiple growth factors in endothelial cells and induced the phosphorylation of Akt and endothelial nitric oxide synthase (eNOS), resulting in enhanced endothelial cell proliferation and migration. Fibroblast growth factors (FGFs) stimulate smooth muscle cell proliferation and migration. The recruitment of endothelial cells and vascular smooth muscle cells (VSMCs) results in arteriogenesis as therapeutic neovascularization. VEGF indicates vascular endothelial growth factor; p-Akt, phosphorylated Akt; p-eNOS; phosphorylated eNOS; EC, endothelial cell.

Ligand-induced activation of PPAR-γ is known to modulate angiogenic factors including VEGF and FGFs via binding to the PPAR response element.[20] Blood flow recovery by Pio-NP was accompanied by arteriogenesis in ischemic hindlimb muscle, which is demonstrated as arterioles with α-smooth muscle actin–positive pericytes. Polymerase chain reaction array revealed that Pio-NP induced multiple genes that are involved in endothelial proliferation and migration (VEGF-A, VEGF-B, VEGF-D, and epidermal growth factor),[21–26] as well as vascular smooth muscle cell migration and proliferation (FGF and Gna13).[27–30] This coordinated induction of endothelial cells and VSMCs is critical for Pio-NP–induced mature arteriogenesis to form functional collaterals.

Recent phase II randomized clinical trials designed to prove the therapeutic neovascularization for ischemic vascular disease by administering exogenous angiogenic growth factors failed to demonstrate the clinical benefits, although each angiogenic growth factor induces angiogenesis (increased capillary density) in preclinical studies.[31,32] Arteriogenesis, defined as the enlargement of preexisting collateral arteries and their remodeling to conductance vessels, is considered to be more effective at inducing blood flow recovery.[33] In the present study, we performed a histological evaluation of the peripheral ischemic muscles and discovered an increased number of endothelial cells (capillaries), as well as smooth muscle cells forming arterioles (Figure 2) along with overall blood flow recovery. These data suggest that neovascularization in the peripheral muscles may induce arteriogenesis in the proximal regions, which remains to be clarified in larger animal models such as rabbits.[11]

eNOS activation appears to be essential for Pio-NP–induced neovascularization, as shown in the experiment using eNOS$^{-/-}$ mice (Figure 4). Several angiogenic factors including VEGF-A, VEGF-B, and FGF are known to activate eNOS phosphorylation in an Akt-dependent and Akt-independent fashion, and the increased endothelium-derived NO in turn mediates the proliferation of endothelial cells,[34–37] which may be a central mechanism of Pio-NP–induced neovascularization (Figure 6). The therapeutic effects afforded by Pio-NP were independent of the improvement in insulin resistance. We demonstrated that the intramuscular injection of Pio-NP did not affect glucose, insulin, or triglyceride levels in the serum. These findings suggest that Pio-NP acted locally on ischemic vascular endothelial cells to induce therapeutic neovascularization.

In conclusion, the NP-mediated endothelial cell–selective delivery of pioglitazone induces functionally mature collaterals through eNOS activation and the expression of multiple endogenous angiogenic growth factors. NP-mediated drug delivery is a novel modality that may advance therapeutic neovascularization over current medical treatment for severe peripheral artery disease, including CLI.

Acknowledgments

We appreciate Eiko Iwata and Miho Miyagawa for their excellent technical assistance.

Disclosures

Dr Egashira holds a patent on the results reported in this study. The remaining authors report no conflict of interest.

References

1. Adam DJ, Beard JD, Cleveland T, Bell J, Bradbury AW, Forbes JF, Fowkes FG, Gillepsie I, Ruckley CV, Raab G, Storkey H; BASIL trial participants. Bypass versus angioplasty in severe ischaemia of the leg (BASIL): multicentre, randomised controlled trial. *Lancet*. 2005;366:1925–1934.
2. Hirsch AT, Haskal ZJ, Hertzer NR, et al. ACC/AHA 2005 Practice Guidelines for the management of patients with peripheral arterial disease (lower extremity, renal, mesenteric, and abdominal aortic): a collaborative report from the American Association for Vascular Surgery/Society for Vascular Surgery, Society for Cardiovascular Angiography and Interventions, Society for Vascular Medicine and Biology, Society of Interventional Radiology, and the ACC/AHA Task Force on Practice Guidelines (Writing Committee to Develop Guidelines for the Management of Patients With Peripheral Arterial Disease): endorsed by the American Association of Cardiovascular and Pulmonary Rehabilitation; National Heart, Lung, and Blood Institute; Society for Vascular Nursing; TransAtlantic Inter-Society Consensus; and Vascular Disease Foundation. *Circulation*. 2006;113:e463–e654.
3. Fukunaga Y, Itoh H, Doi K, Tanaka T, Yamashita J, Chun TH, Inoue M, Masatsugu K, Sawada N, Saito T, Hosoda K, Kook H, Ueda M, Nakao K. Thiazolidinediones, peroxisome proliferator-activated receptor gamma agonists, regulate endothelial cell growth and secretion of vasoactive peptides. *Atherosclerosis*. 2001;158:113–119.
4. Gensch C, Clever YP, Werner C, Hanhoun M, Böhm M, Laufs U. The PPAR-gamma agonist pioglitazone increases neoangiogenesis and prevents apoptosis of endothelial progenitor cells. *Atherosclerosis*. 2007;192:67–74.
5. Murata T, He S, Hangai M, Ishibashi T, Xi XP, Kim S, Hsueh WA, Ryan SJ, Law RE, Hinton DR. Peroxisome proliferator-activated receptor-gamma ligands inhibit choroidal neovascularization. *Invest Ophthalmol Vis Sci*. 2000;41:2309–2317.
6. Chu K, Lee ST, Koo JS, Jung KH, Kim EH, Sinn DI, Kim JM, Ko SY, Kim SJ, Song EC, Kim M, Roh JK. Peroxisome proliferator-activated

receptor-gamma-agonist, rosiglitazone, promotes angiogenesis after focal cerebral ischemia. *Brain Res*. 2006;1093:208–218.
7. Panigrahy D, Singer S, Shen LQ, Butterfield CE, Freedman DA, Chen EJ, Moses MA, Kilroy S, Duensing S, Fletcher C, Fletcher JA, Hlatky L, Hahnfeldt P, Folkman J, Kaipainen A. PPARgamma ligands inhibit primary tumor growth and metastasis by inhibiting angiogenesis. *J Clin Invest*. 2002;110:923–932.
8. Biscetti F, Gaetani E, Flex A, Aprahamian T, Hopkins T, Straface G, Pecorini G, Stigliano E, Smith RC, Angelini F, Castellot JJ Jr, Pola R. Selective activation of peroxisome proliferator-activated receptor (PPAR)alpha and PPAR gamma induces neoangiogenesis through a vascular endothelial growth factor-dependent mechanism. *Diabetes*. 2008;57:1394–1404.
9. Huang PH, Sata M, Nishimatsu H, Sumi M, Hirata Y, Nagai R. Pioglitazone ameliorates endothelial dysfunction and restores ischemia-induced angiogenesis in diabetic mice. *Biomed Pharmacother*. 2008;62:46–52.
10. Kubo M, Egashira K, Inoue T, Koga J, Oda S, Chen L, Nakano K, Matoba T, Kawashima Y, Hara K, Tsujimoto H, Sueishi K, Tominaga R, Sunagawa K. Therapeutic neovascularization by nanotechnology-mediated cell-selective delivery of pitavastatin into the vascular endothelium. *Arterioscler Thromb Vasc Biol*. 2009;29:796–801.
11. Oda S, Nagahama R, Nakano K, Matoba T, Kubo M, Sunagawa K, Tominaga R, Egashira K. Nanoparticle-mediated endothelial cell-selective delivery of pitavastatin induces functional collateral arteries (therapeutic arteriogenesis) in a rabbit model of chronic hind limb ischemia. *J Vasc Surg*. 2010;52:412–420.
12. Kawashima Y, Yamamoto H, Takeuchi H, Hino T, Niwa T. Properties of a peptide containing DL-lactide/glycolide copolymer nanospheres prepared by novel emulsion solvent diffusion methods. *Eur J Pharm Biopharm*. 1998;45:41–48.
13. Lamalice L, Le Boeuf F, Huot J. Endothelial cell migration during angiogenesis. *Circ Res*. 2007;100:782–794.
14. Yuen CY, Wong WT, Tian XY, Wong SL, Lau CW, Yu J, Tomlinson B, Yao X, Huang Y. Telmisartan inhibits vasoconstriction via PPAR?-dependent expression and activation of endothelial nitric oxide synthase. *Cardiovasc Res*. 2011;90:122–129.
15. Calnek DS, Mazzella L, Roser S, Roman J, Hart CM. Peroxisome proliferator-activated receptor gamma ligands increase release of nitric oxide from endothelial cells. *Arterioscler Thromb Vasc Biol*. 2003;23:52–57.
16. Margeli A, Kouraklis G, Theocharis S. Peroxisome proliferator activated receptor-gamma (PPAR-gamma) ligands and angiogenesis. *Angiogenesis*. 2003;6:165–169.
17. Guan Y, Hao C, Cha DR, Rao R, Lu W, Kohan DE, Magnuson MA, Redha R, Zhang Y, Breyer MD. Thiazolidinediones expand body fluid volume through PPARgamma stimulation of ENaC-mediated renal salt absorption. *Nat Med*. 2005;11:861–866.
18. Tseng CH. Pioglitazone and bladder cancer in human studies: is it diabetes itself, diabetes drugs, flawed analyses or different ethnicities? *J Formos Med Assoc*. 2012;111:123–131.
19. Danhier F, Ansorena E, Silva JM, Coco R, Le Breton A, Préat V. PLGA-based nanoparticles: An overview of biomedical applications. *J Control Release*. 2012;161:505–522.
20. Cho DH, Choi YJ, Jo SA, Jo I. Nitric oxide production and regulation of endothelial nitric-oxide synthase phosphorylation by prolonged treatment with troglitazone: evidence for involvement of peroxisome proliferator-activated receptor (PPAR) gamma-dependent and PPARgamma-independent signaling pathways. *J Biol Chem*. 2004;279:2499–2506.
21. Silvestre JS, Tamarat R, Ebrahimian TG, Le-Roux A, Clergue M, Emmanuel F, Duriez M, Schwartz B, Branellec D, Lévy BI. Vascular endothelial growth factor-B promotes in vivo angiogenesis. *Circ Res*. 2003;93:114–123.
22. Im E, Kazlauskas A. Regulating angiogenesis at the level of PtdIns-4,5-P2. *EMBO J*. 2006;25:2075–2082.
23. Matsumoto T, Claesson-Welsh L. VEGF receptor signal transduction. *Sci STKE*. 2001;2001:re21.
24. Rahimi N. VEGFR-1 and VEGFR-2: two non-identical twins with a unique physiognomy. *Front Biosci*. 2006;11:818–829.
25. Normanno N, De Luca A, Bianco C, Strizzi L, Mancino M, Maiello MR, Carotenuto A, De Feo G, Caponigro F, Salomon DS. Epidermal growth factor receptor (EGFR) signaling in cancer. *Gene*. 2006;366:2–16.
26. Jauhiainen S, Häkkinen SK, Toivanen PI, Heinonen SE, Jyrkkänen HK, Kansanen E, Leinonen H, Levonen AL, Ylä-Herttuala S. Vascular endothelial growth factor (VEGF)-D stimulates VEGF-A, stanniocalcin-1, and neuropilin-2 and has potent angiogenic effects. *Arterioscler Thromb Vasc Biol*. 2011;31:1617–1624.
27. Doukas J, Blease K, Craig D, Ma C, Chandler LA, Sosnowski BA, Pierce GF. Delivery of FGF genes to wound repair cells enhances arteriogenesis and myogenesis in skeletal muscle. *Mol Ther*. 2002;5:517–527.
28. Ghiselli G, Chen J, Kaou M, Hallak H, Rubin R. Ethanol inhibits fibroblast growth factor-induced proliferation of aortic smooth muscle cells. *Arterioscler Thromb Vasc Biol*. 2003;23:1808–1813.
29. Offermanns S, Mancino V, Revel JP, Simon MI. Vascular system defects and impaired cell chemokinesis as a result of Galpha13 deficiency. *Science*. 1997;275:533–536.
30. Boilly B, Vercoutter-Edouart AS, Hondermarck H, Nurcombe V, Le Bourhis X. FGF signals for cell proliferation and migration through different pathways. *Cytokine Growth Factor Rev*. 2000;11:295–302.
31. Losordo DW, Dimmeler S. Therapeutic angiogenesis and vasculogenesis for ischemic disease. Part I: angiogenic cytokines. *Circulation*. 2004;109:2487–2491.
32. van Royen N, Piek JJ, Schaper W, Fulton WF. A critical review of clinical arteriogenesis research. *J Am Coll Cardiol*. 2009;55:17–25.
33. Schaper W, Scholz D. Factors regulating arteriogenesis. *Arterioscler Thromb Vasc Biol*. 2003;23:1143–1151.
34. Hayakawa H, Hirata Y, Kakoki M, Suzuki Y, Nishimatsu H, Nagata D, Suzuki E, Kikuchi K, Nagano T, Kangawa K, Matsuo H, Sugimoto T, Omata M. Role of nitric oxide-cGMP pathway in adrenomedullin-induced vasodilation in the rat. *Hypertension*. 1999;33:689–693.
35. Murohara T, Asahara T, Silver M, Bauters C, Masuda H, Kalka C, Kearney M, Chen D, Symes JF, Fishman MC, Huang PL, Isner JM. Nitric oxide synthase modulates angiogenesis in response to tissue ischemia. *J Clin Invest*. 1998;101:2567–2578.
36. Ziche M, Morbidelli L, Choudhuri R, Zhang HT, Donnini S, Granger HJ, Bicknell R. Nitric oxide synthase lies downstream from vascular endothelial growth factor-induced but not basic fibroblast growth factor-induced angiogenesis. *J Clin Invest*. 1997;99:2625–2634.
37. Duval M, Le Boeuf F, Huot J, Gratton JP. Src-mediated phosphorylation of Hsp90 in response to vascular endothelial growth factor (VEGF) is required for VEGF receptor-2 signaling to endothelial NO synthase. *Mol Biol Cell*. 2007;18:4659–4668.

Supplementary Figure Legends

Supplementary Figure I. Animal experimental protocols.

In protocol 1, the treatment groups received intramuscular injections of FITC-NP (0.9 mg/100 μl PLGA; NP group), pioglitazone at 0.0025, 0.025 μg/100 μl (1 μg/kg; pioglitazone group), or pioglitazone-NP (0.067, 0.67 μg/100 μl PLGA containing 0.0025, 0.025 μg pioglitazone) into the left femoral and thigh muscles using a 27-gauge needle. In protocol 2, the effects of the intramuscular injections of pioglitazone-NP were examined in wild-type mice administered GW9662 (PPAR-γ antagonist) (Sigma). In protocol 3, the effects of the intramuscular injections of pioglitazone-NP were examined in endothelial nitric oxide synthase (eNOS) $^{-/-}$ mice. WT mice or eNOS$^{-/-}$ mice received single intramuscular injections of pioglitazone-NP at doses of 1 μg/kg immediately after inducing ischemia. In protocol 4, immediately after inducing ischemia, the animals were randomly divided into three groups; three other groups received a systemic daily oral administration of pioglitazone at doses of 1, 500 and 1000 μg/kg dissolved in 0.5% carboxymethyl cellulose by gavage from the day of surgery until the mice were euthanized on day 21.

Supplementary Figure II. Cellular distribution of NP in ischemic muscles.

A, Representative light (upper panels) and fluorescent (lower panels) stereomicrographs of the gastrocnemius muscles isolated from a control, non-ischemic hindlimb and those from an ischemic hindlimb injected with FITC-NP or FITC alone. B, Quantitative analysis of the magnitude of intracellular FITC fluorescence signals in the gastrocnemius muscles are shown. The data were compared using two-way ANOVA followed by Bonferroni's multiple comparison tests. *$p<0.05$ versus control condition. $^{\dagger}p<0.05$ versus FITC. C, Immunofluorescent staining of cross-sections from ischemic muscle 3 days after a FITC-NP or FITC only injection stained with the endothelial marker CD31 (red). Scale bars: 100 μm.

Supplemental Table I. Serum concentration of glucose, triglyceride and insulin at 3 weeks after daily oral administration of pioglitazone

Oral Pioglitazone (mg/kg/day)	Body Weight (g)	Serum Glucose (mg/dL)	Serum Triglyceride (mg/dL)	Serum Insulin (μIU/mL)
0	24.4±0.6	303±33	39±2	ND
1	24.5±1.0	272±23	55±11	ND
500	24.4±1.2	309±114	60±12	ND
1000	23.6±0.9	280±48	63±10	ND

ND: not detected (<0.3 μIU/mL)

The data are shown as the mean±SEM (n=2-5 each).